

# Milagrito Moon Shadow Update

Anthony Shoup

Dept. of Physics  
University of California  
Irvine, CA 92717

April 7, 1997

## 1 Introduction

This is an update on the status of my moon analysis. It is based on about a factor of 3 increase in statistics. It also includes using the correct geographic coordinates for the Milagro site. Previous results used the coordinates of Cygnus as Bob Ellsworth pointed out (old bugs die hard). The error in coordinates introduced a systematic shift of about 0.4 degrees in RA to the east (larger RA). Using the same data set as my first memo and the correct geographic coordinates, I obtained the same results as the last row in Table II in that memo ( $\sigma_{res} = 0.36^{+0.09}_{-0.06}$ ,  $\Delta\alpha = -0.11$ ,  $\Delta\delta = -0.23$ ,  $N_\sigma = 3.2$ ) except that  $\Delta\alpha$  changed to -0.57.

The increase in statistics has allowed me to further explore the dependence of the shadow on NFit (the number of pmts in the fit) and on  $\theta_m$ , cut on zenith angle of the moon. Gaurang Yodh's memo indicates that there still may be significant geomagnetic deflections of the shower primaries even with a  $\theta_m$  cut of  $45^\circ$ .

The data stripping and fitting methods are the same as before with the exception that I have introduced a chi-squared per degree of freedom cut of 30.0 to remove statistically poor fits. This cut loses about 15% of events in the all data set and about 2% of events with  $NFit \geq 50$ .

We currently have almost half a million events within  $5^\circ$  of the moon. The "stripped" summary files are about 220 MB of data and the "stripped" processed+cal data files are about 8.7 GB. The data span the Julian days from 2450504.5 to 2450543.5 (2/21/97 to 4/5/97), although there were several moon transits where little if any data was collected. Run 50 had the largest number of events, 39,934 with  $5^\circ$ , although only 3896 were when  $\theta_m \geq 45^\circ$ .

## 2 Results

Figure 1 shows the cumulative significance of the moon shadow vs time (increasing runs) for all events where  $\theta_m \geq 45^\circ$ . The flat area centered on relative run 20 is during the time when the water on top of the pond was the deepest and the trigger rate was the lowest. The sharp rise at relative run 27 is about where the water was pumped off the pond. This could be an indication that the curvature part of our slewing corrections needs changed for this operating condition. Overall, the significance of the moon shadow is continuing to increase.

The details of the fitting results are summarized in Tables I & II below. Table I listed the results using all available runs while Table II results are excluding runs 50-59 (the flat area in Figure 1). I have also included all figures showing density and deficit plots for each data set in the tables. Figure a for each set is the density plot and figure b is the deficit plot. These figures are not for the faint of heart. The statistics are fairly low in some of them and the errors in the deficit plots are correlated. The figure numbers are tabulated in the tables. These results show:

1. We are starting to have enough data to see the moon shadow for all events even with the degradation of the geomagnetic field.
2. There is some evidence that even with a  $\theta_m \geq 45^\circ$  cut there is still some degrading of the moon shadow by the geomagnetic field. The resolution for events for  $\theta_m \geq 60^\circ$  is better than that for the  $45^\circ$  cut, although only by about one sigma.
3. There is evidence that the resolution does improve with increasing NFit (# of pmts in fit), although more statistics are needed

to confirm this.

4. The shape of the shadow is not too far from a 2-D Gaussian. The ratios of  $\frac{\sigma_{72}}{\sigma_{res}}$  ( $\sigma_{72}$  is the angular distance where 72% of the deficit is obtained) are generally close to the expected value of 1.58. Large deviations are typically caused by  $\sigma_{72}$  being smaller (or that  $\sigma_{res}$  is larger) than expected.
5. The data is not shown, but my results of allowing offsets in both RA and DEC to vary in the fits yields no significant effect ( $< 0.5$  sigma).

### 3 Future

I have stopped reconstructing data using my offline program since the online reconstruction has begun. I will continue to accumulate data on the moon and hope to confirm a shadow using the online reconstruction results.

With future increases in statistics it should be possible to further explore and more accurately extract our true angular resolution from the apparent moon shadow.

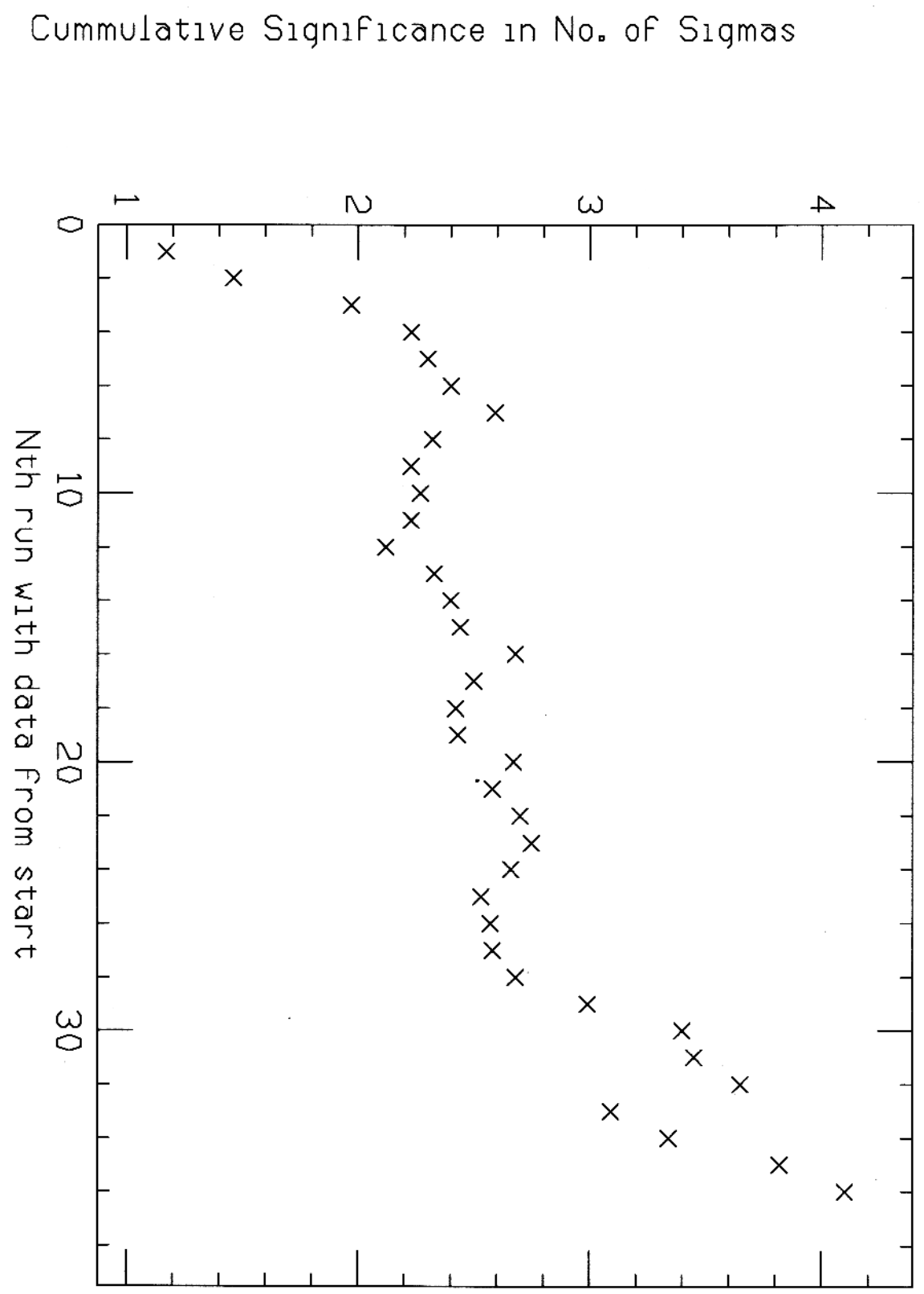
Table I. Shadow Fit Results using Runs: 12-30, 50-59, 61-63, 65-68, 71, 74

$\theta_m$	NFit	# Events	$\sigma_{res}$	$N_\sigma$	$\sigma_{72}$	$\frac{\sigma_{72}}{\sigma_{res}}$	Figure #
00-90	all	430249	$1.6^{+0.5}_{-0.4}$	2.47	2.56	1.60	2
00-90	$\geq 50$	267242	$1.5^{+0.5}_{-0.3}$	2.59	2.44	1.63	3
00-90	$\geq 75$	136520	$1.5^{+0.9}_{-0.5}$	1.71	2.56	1.71	4
45-90	all	133261	$0.66^{+0.15}_{-0.11}$	4.10	1.06	1.61	5
45-90	$\geq 50$	73043	$0.58^{+0.16}_{-0.11}$	4.16	0.56	0.96	6
45-90	$\geq 75$	33359	$0.61^{+0.28}_{-0.16}$	3.03	0.56	0.92	7
60-90	all	24881	$0.58^{+0.39}_{-0.24}$	2.07	0.81	1.40	8
60-90	$\geq 50$	10088	$0.83^{+0.65}_{-0.33}$	1.70	0.81	0.97	9

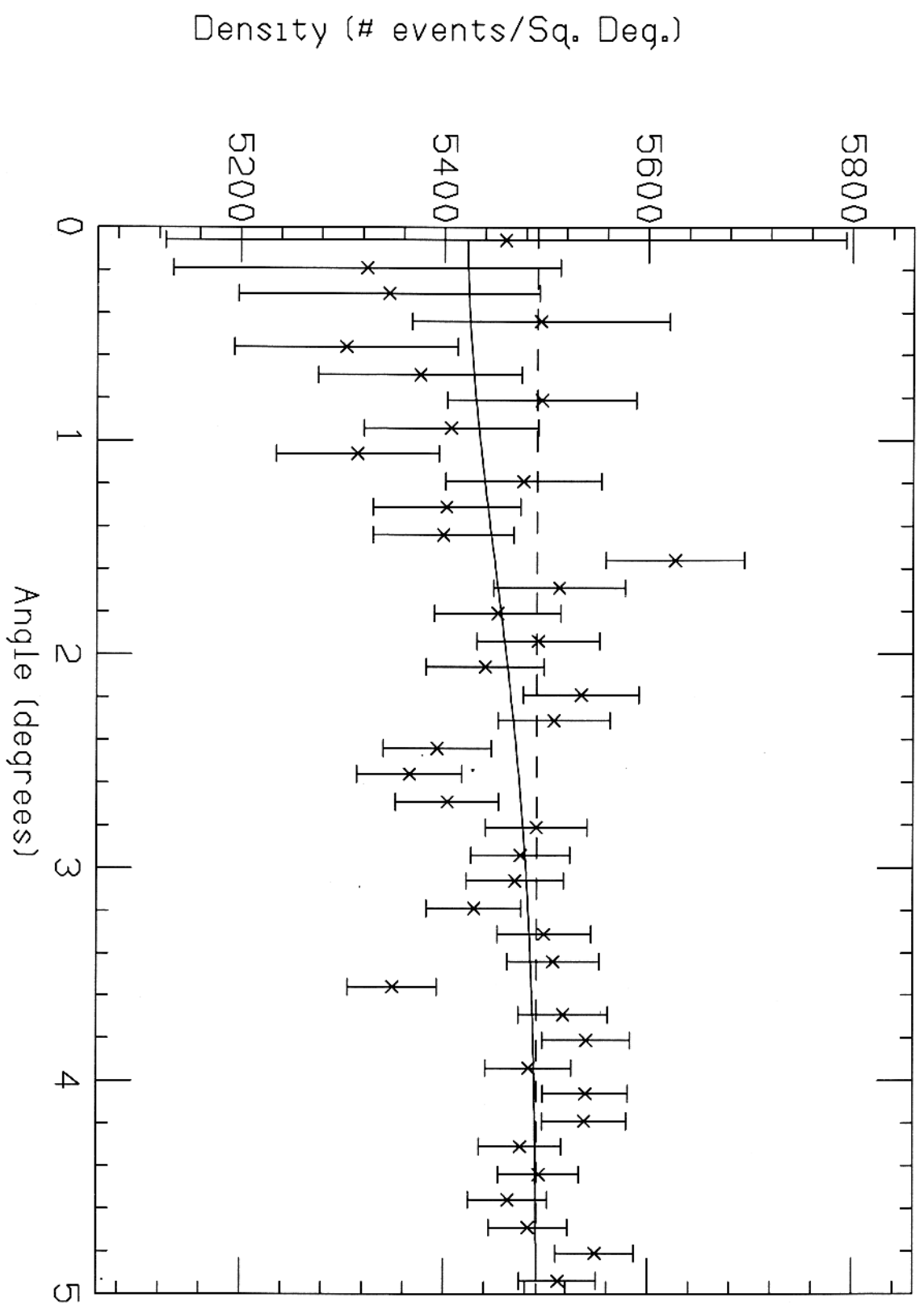
Table II. Shadow Fit Results using Runs: 12-30, 61-63, 65-68, 71, 74

$\theta_m$	NFit	# Events	$\sigma_{res}$	$N_\sigma$	$\sigma_{72}$	$\frac{\sigma_{72}}{\sigma_{res}}$	Figure #
00-90	all	237059	$1.3^{+0.5}_{-0.4}$	2.34	1.44	1.11	10
00-90	$\geq 50$	147158	$1.3^{+0.6}_{-0.5}$	2.44	1.31	1.01	11
00-90	$\geq 75$	74868	$1.5^{+1.0}_{-0.8}$	1.51	2.08	1.39	12
45-90	all	106028	$0.64^{+0.17}_{-0.12}$	3.95	0.94	1.47	13
45-90	$\geq 50$	60389	$0.45^{+0.13}_{-0.08}$	4.36	0.56	1.24	14
45-90	$\geq 75$	27781	$0.52^{+0.24}_{-0.14}$	3.12	0.56	1.08	15
60-90	all	19019	$0.28^{+0.11}_{-0.05}$	2.64	0.81	2.89	16
60-90	$\geq 50$	8281	$0.64^{+0.53}_{-0.41}$	1.95	0.44	0.69	17

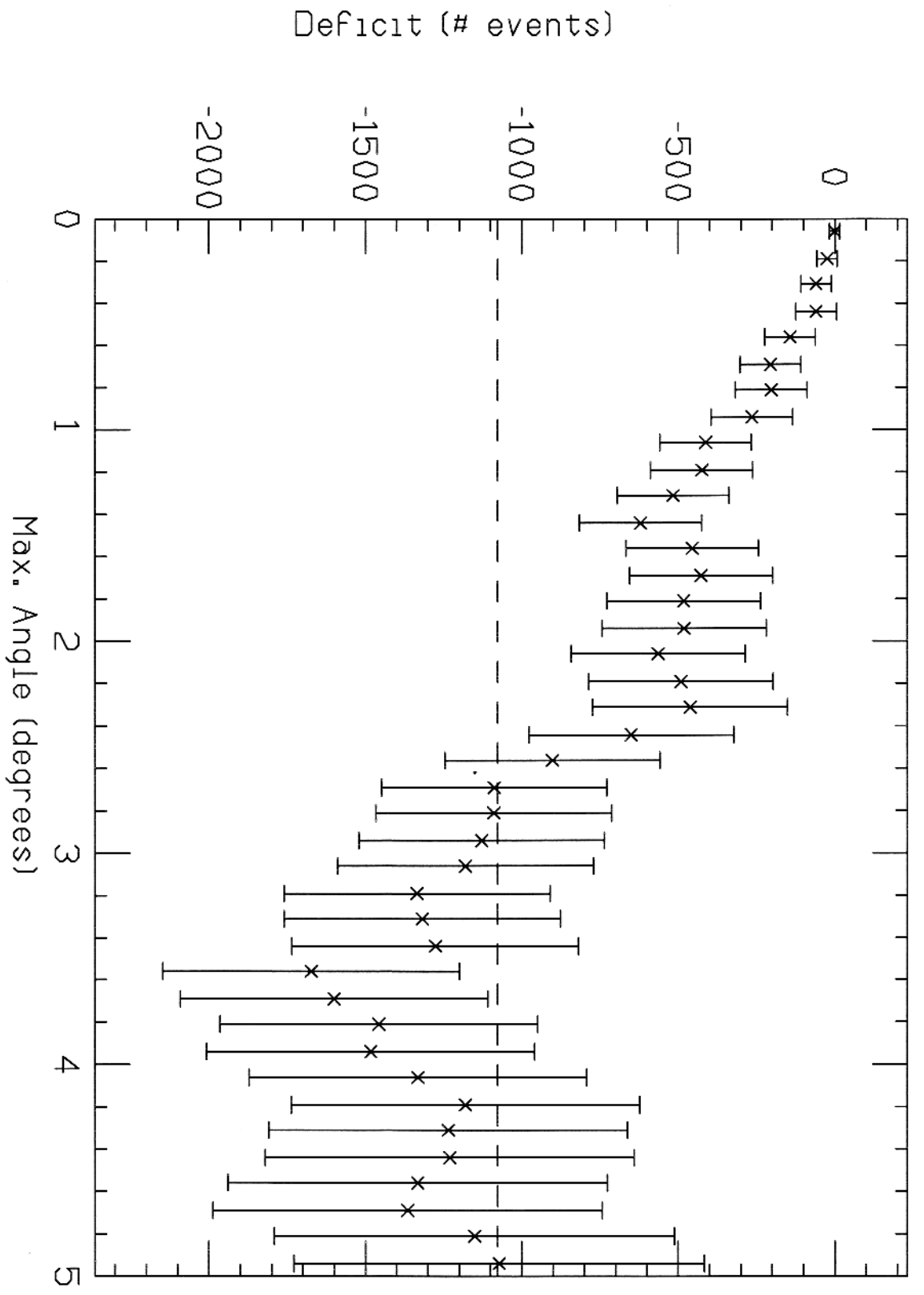
Significance of Moon Shadow (Figure 1)



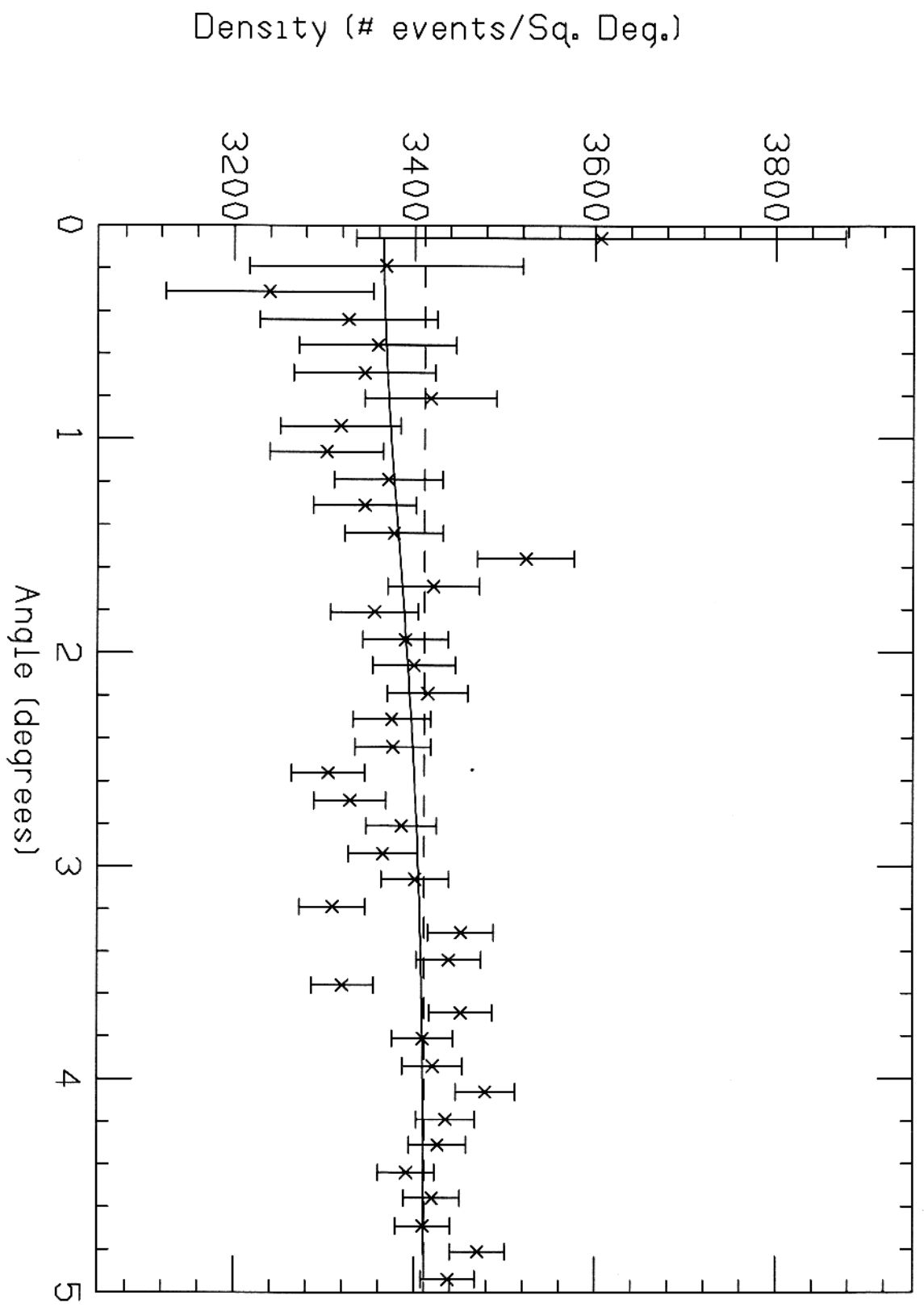
Density vs. Angle (Figure 2a)



Deficit vs. Max. Angle (Figure 2b)

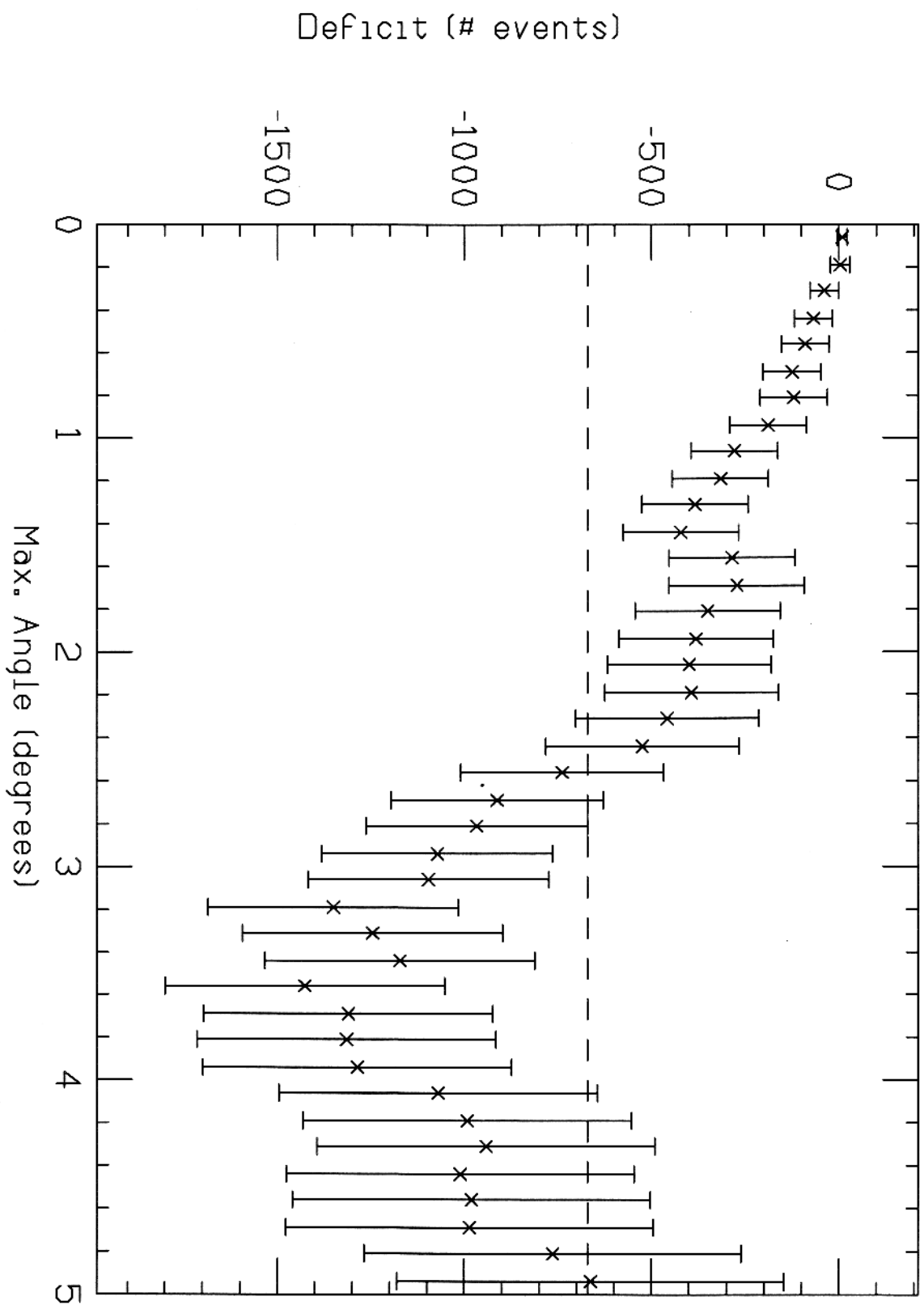


Density vs. Angle (Figure 3a)

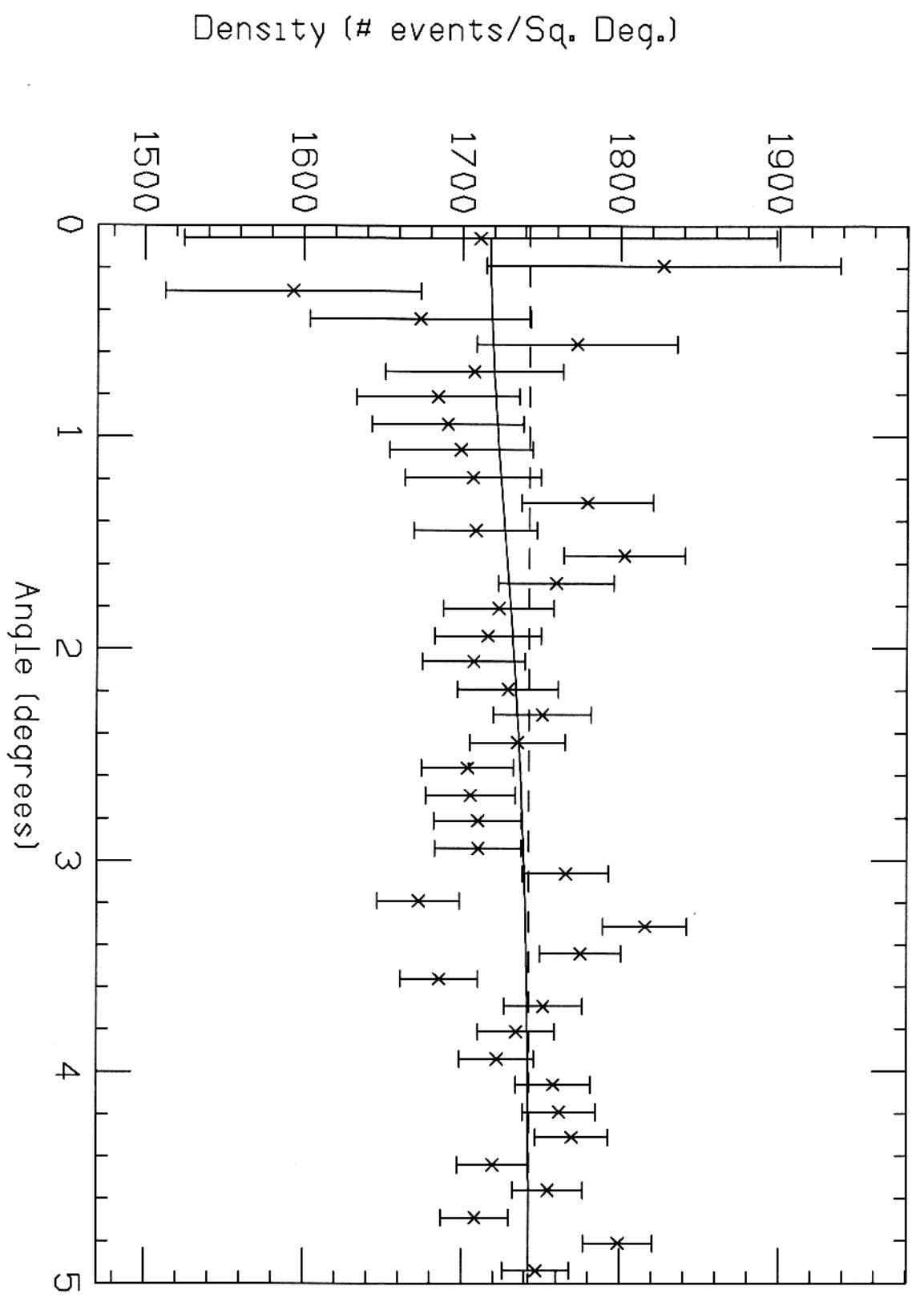




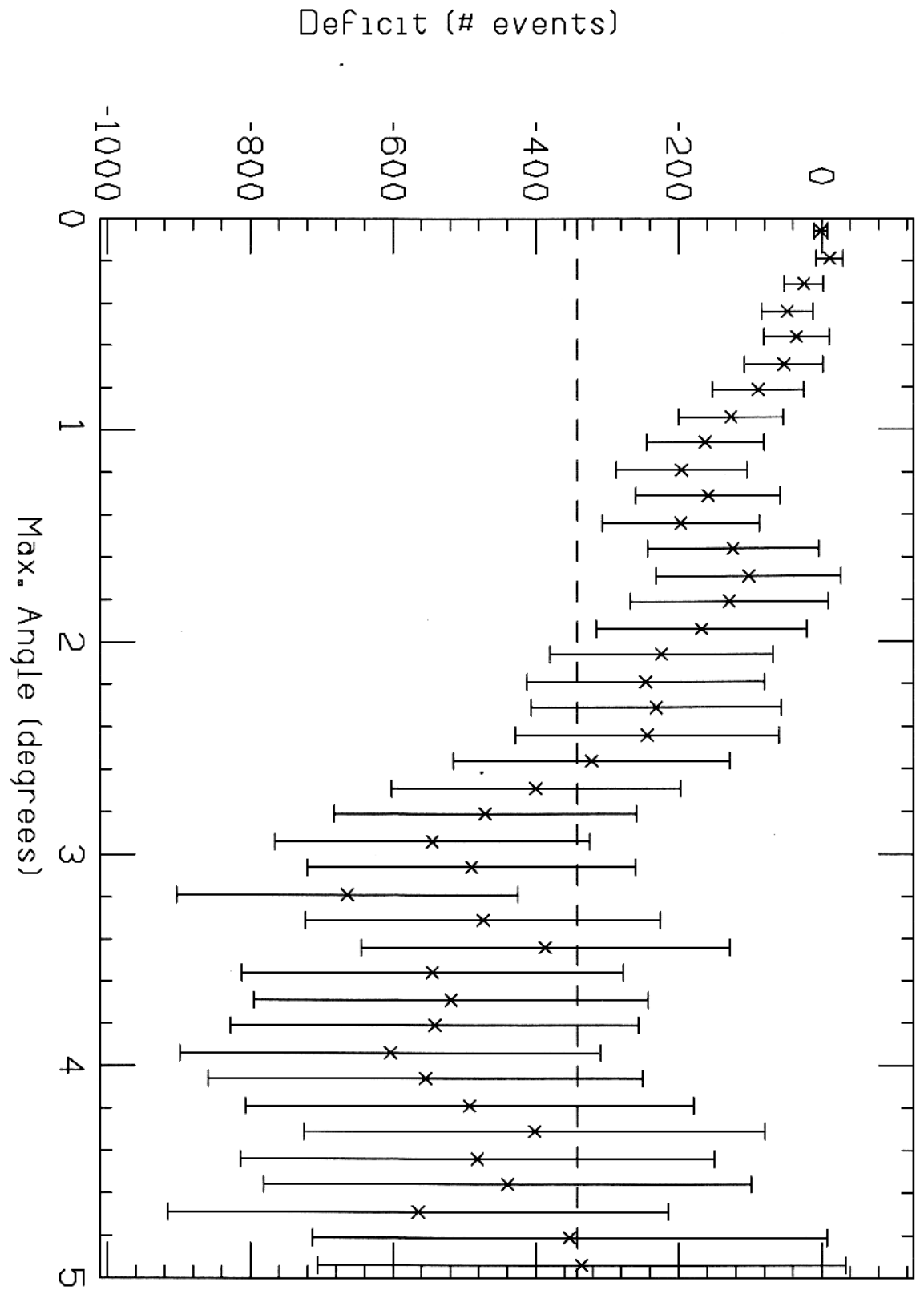
Deficit vs. Max. Angle (Figure 3b)



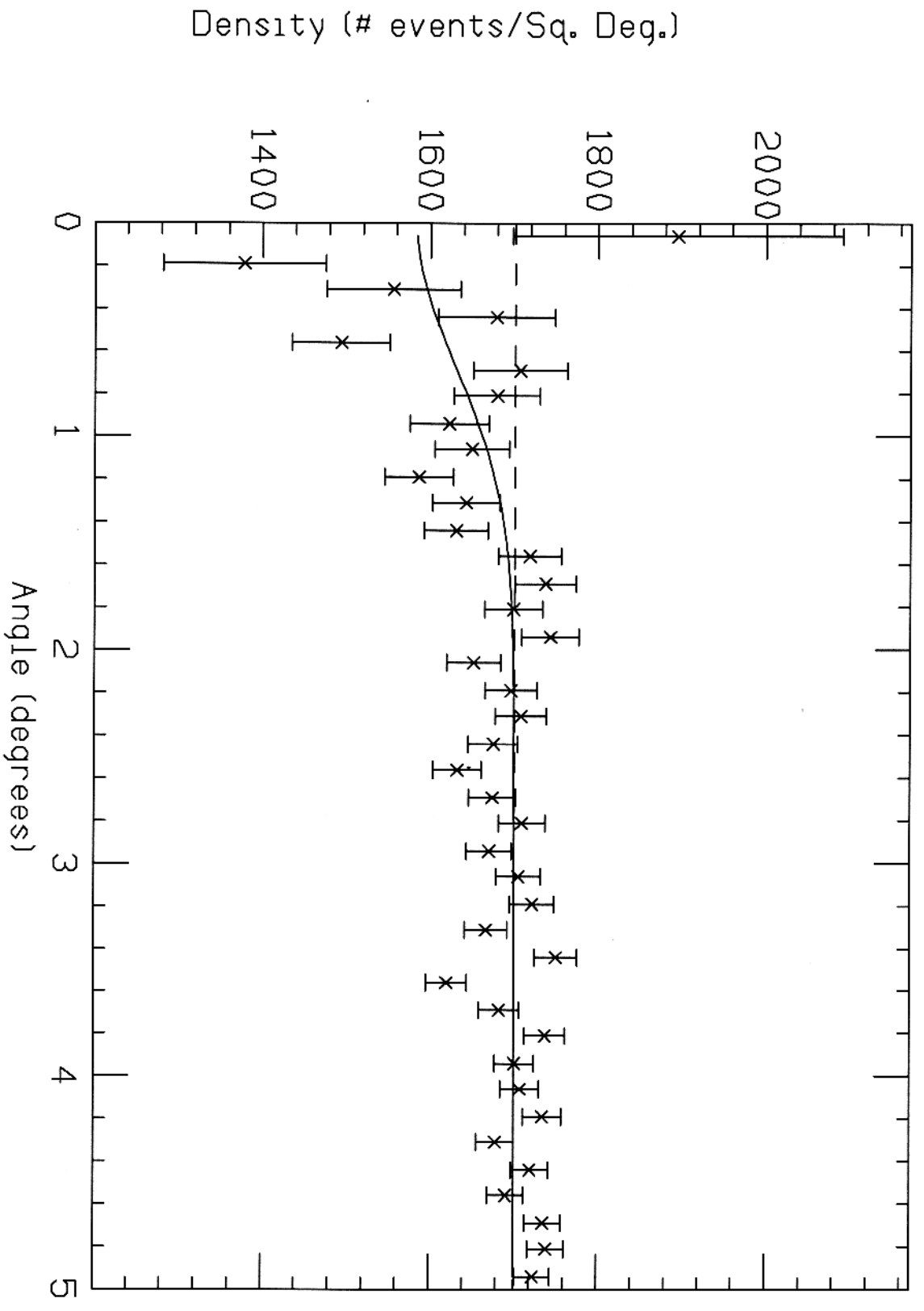
Density vs. Angle (Figure 4a)



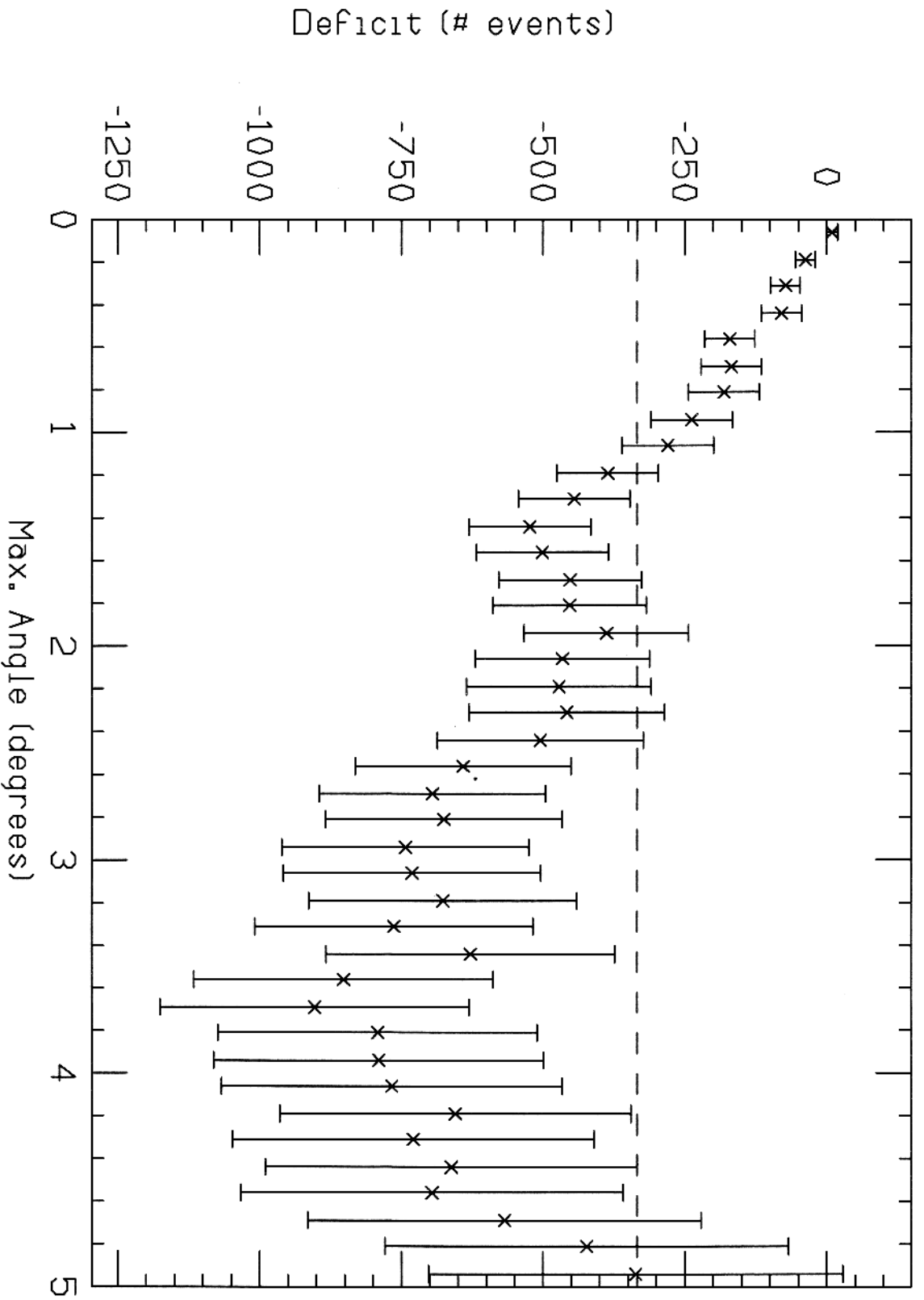
Deficit vs. Max. Angle (Figure 4b)



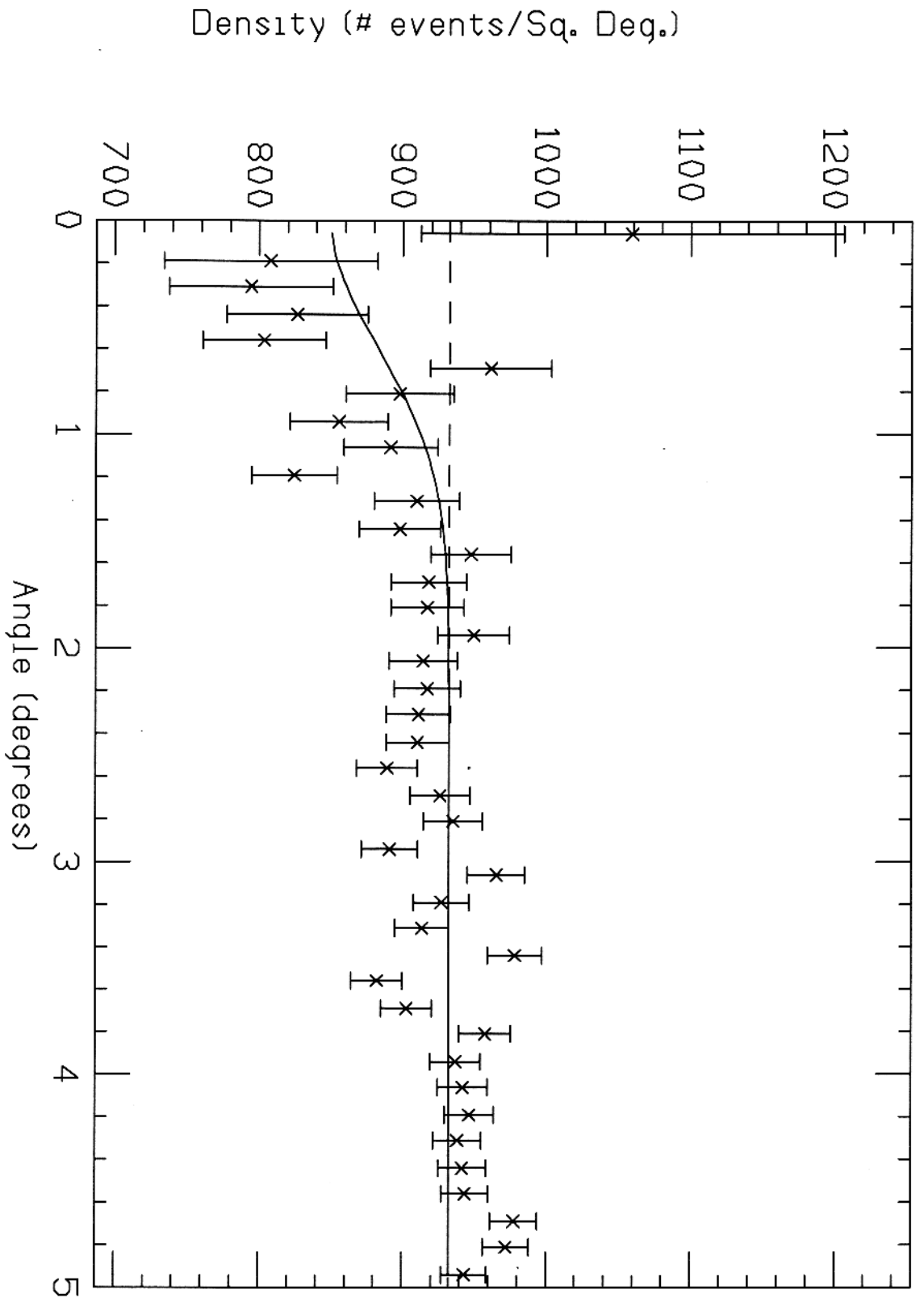
Density vs. Angle (Figure 5a)



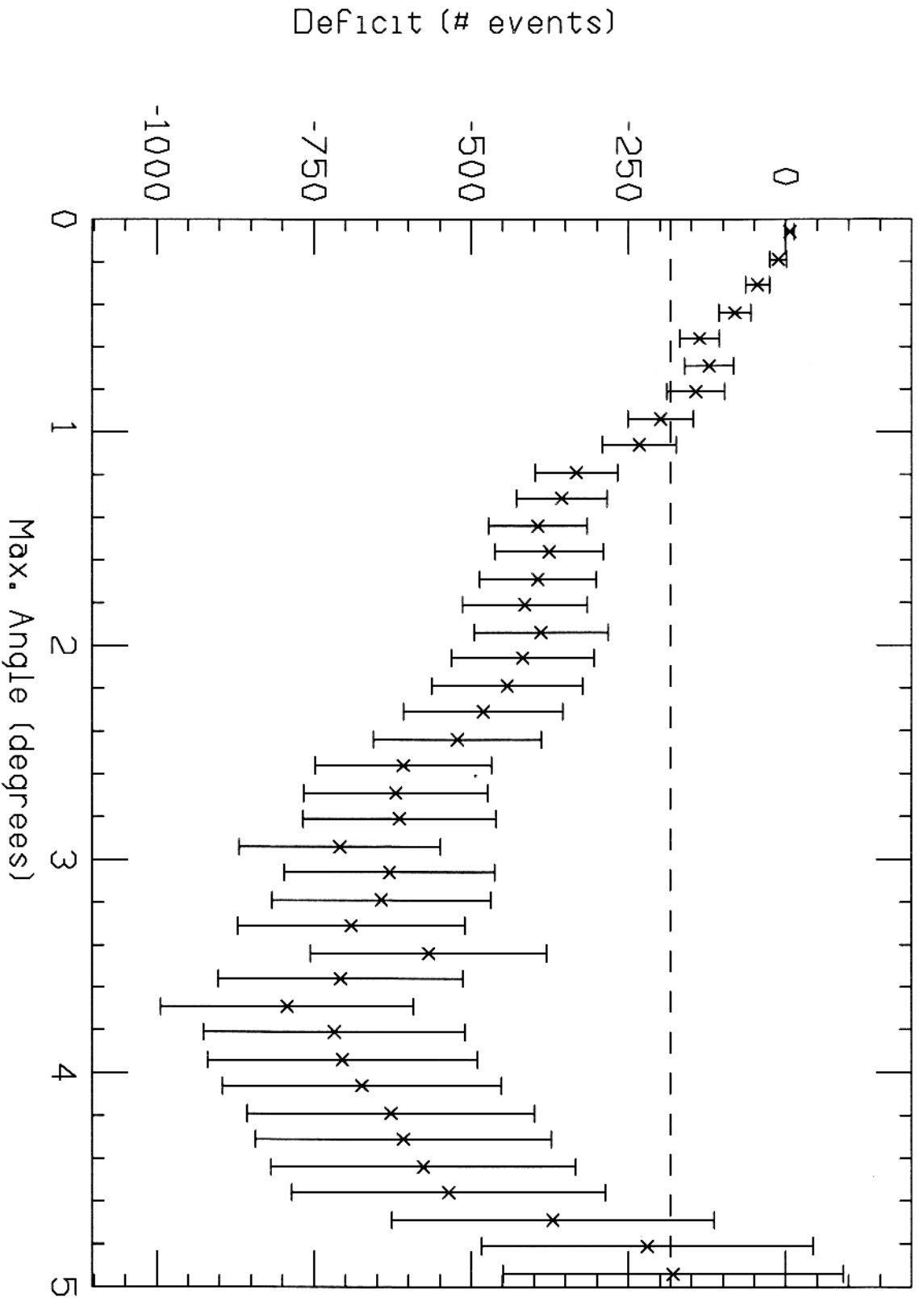
Deficit vs. Max. Angle (Figure 5b)



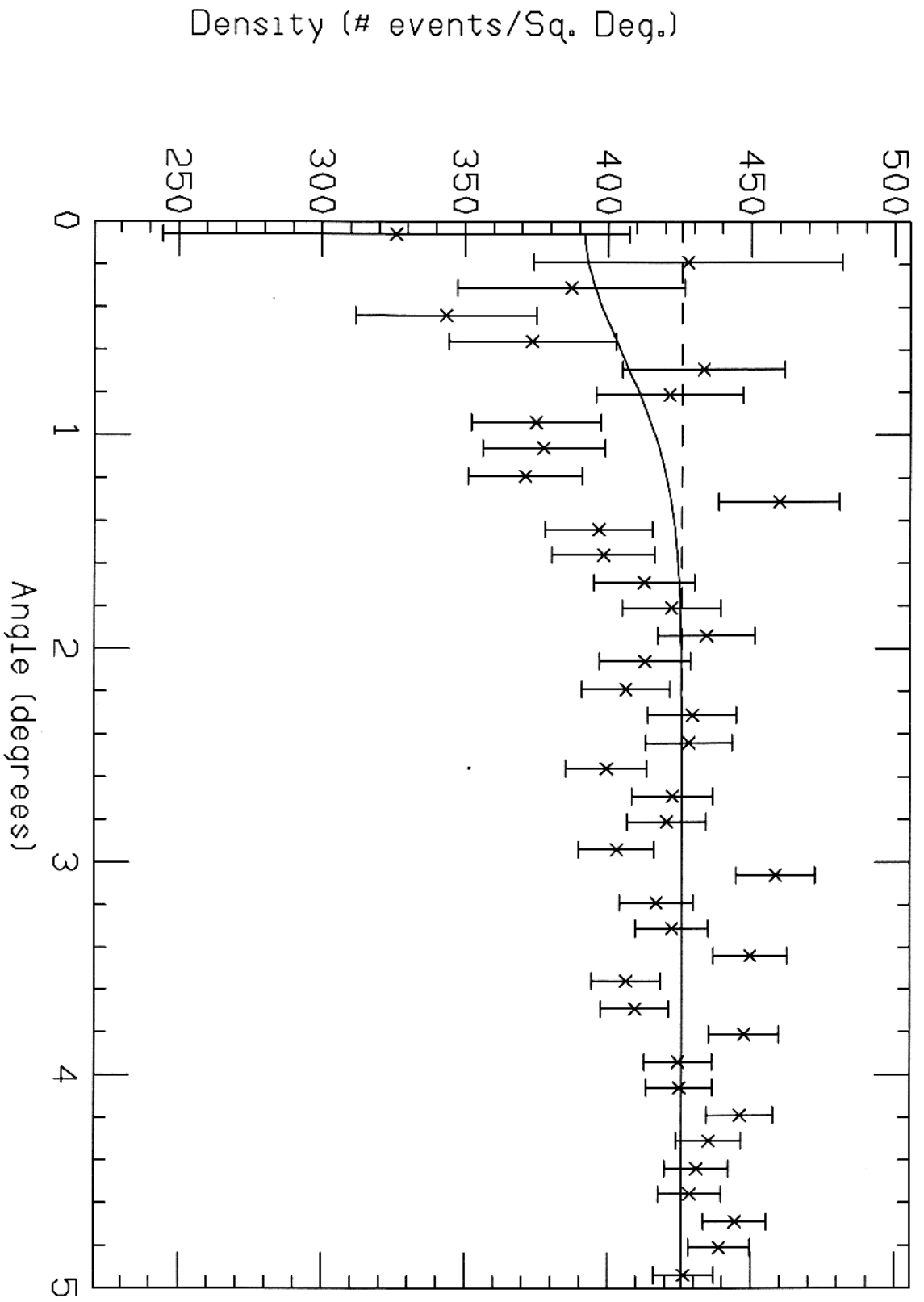
Density vs. Angle (Figure 6a)



Deficit vs. Max. Angle (Figure 6b)

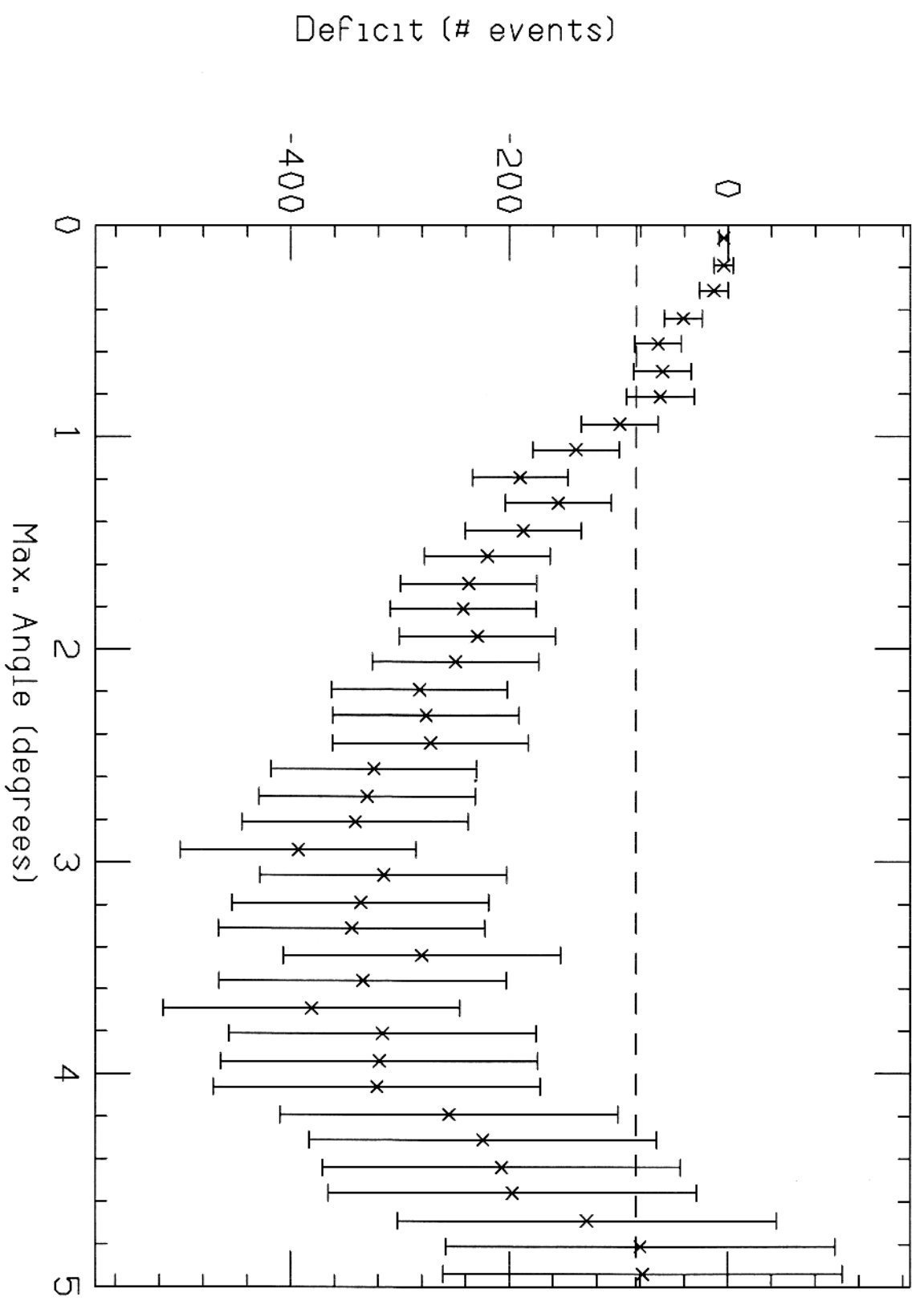


Density vs. Angle (Figure 7a)

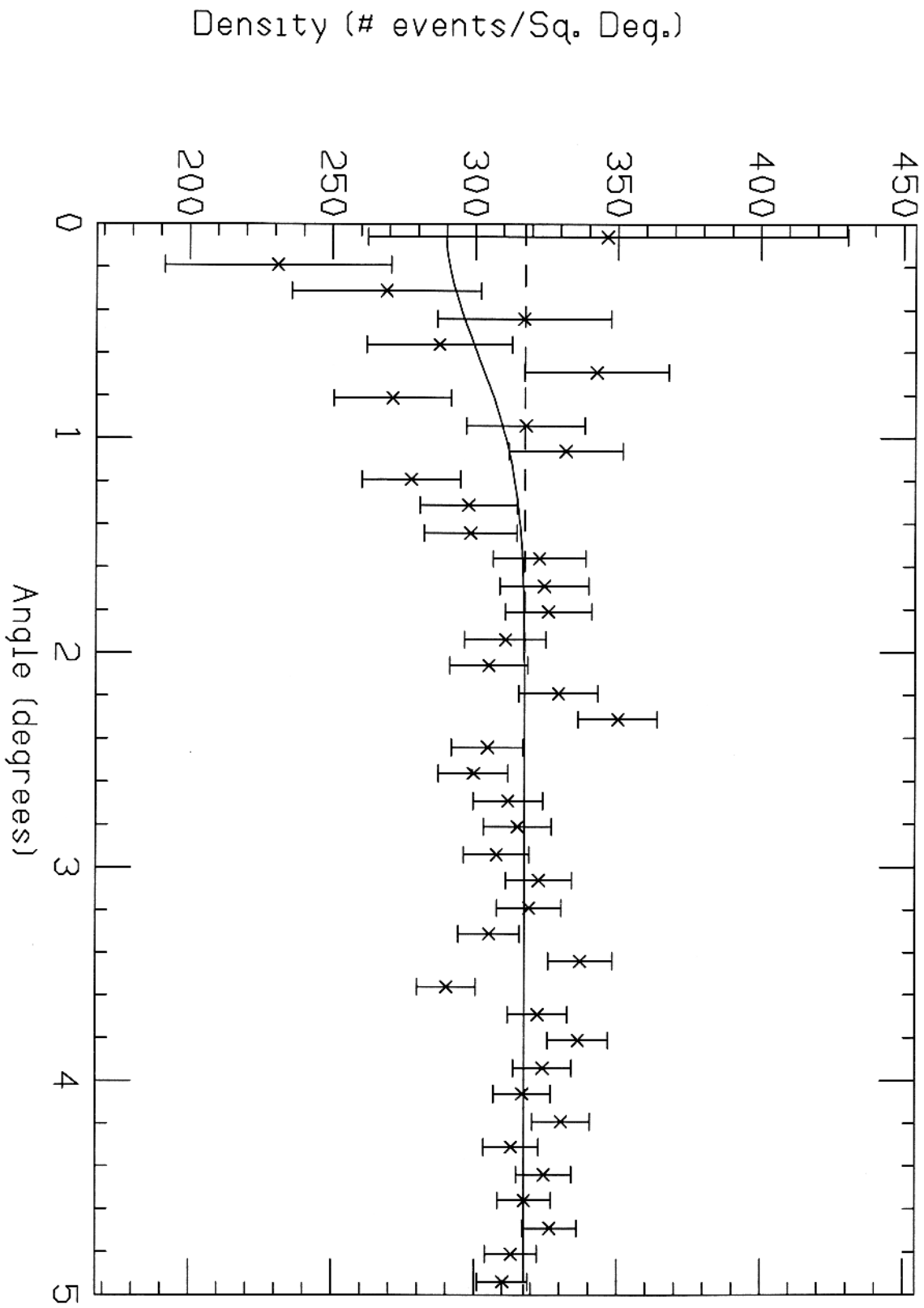




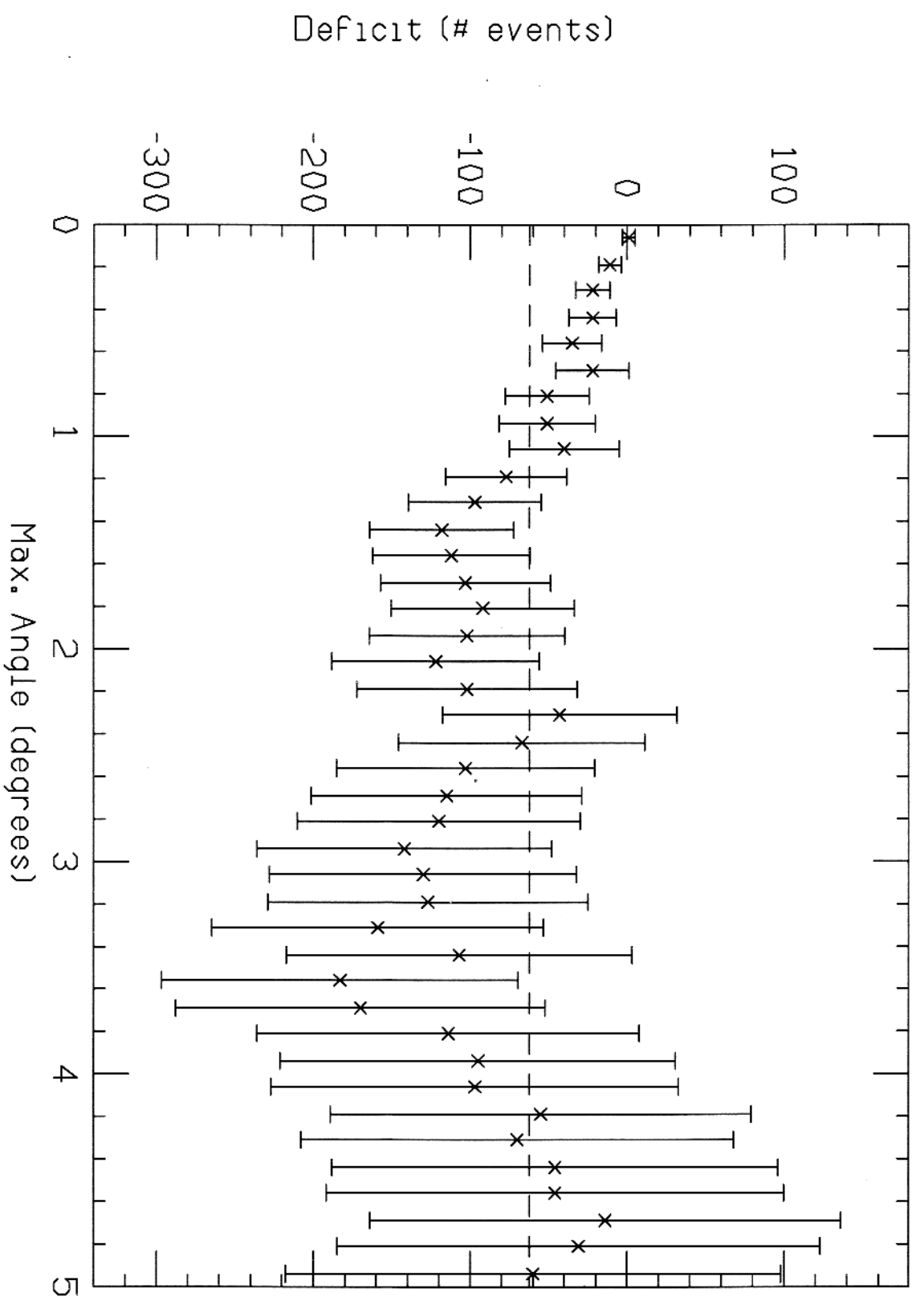
Deficit vs. Max. Angle (Figure 7b)



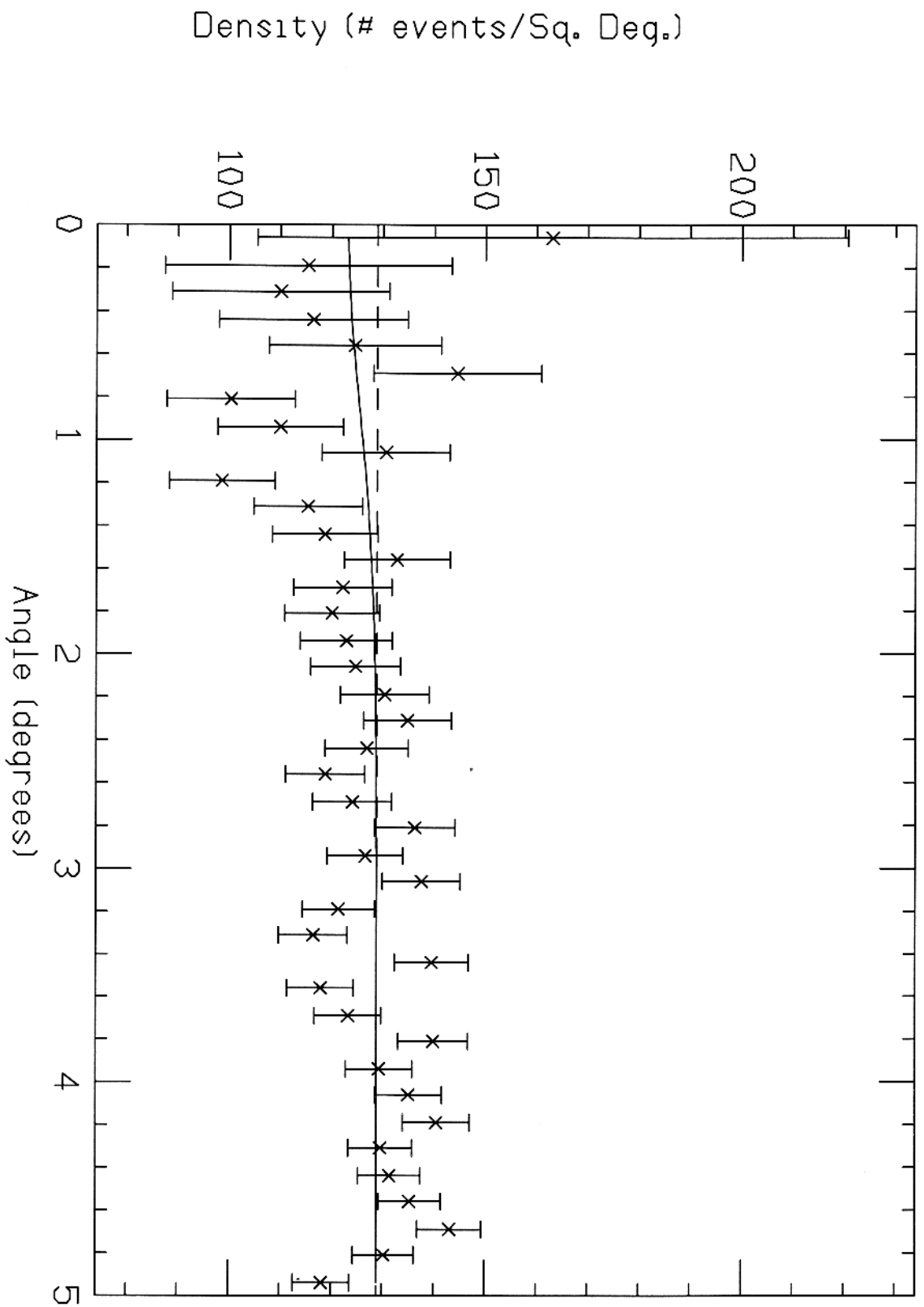
Density vs. Angle (Figure 8a)



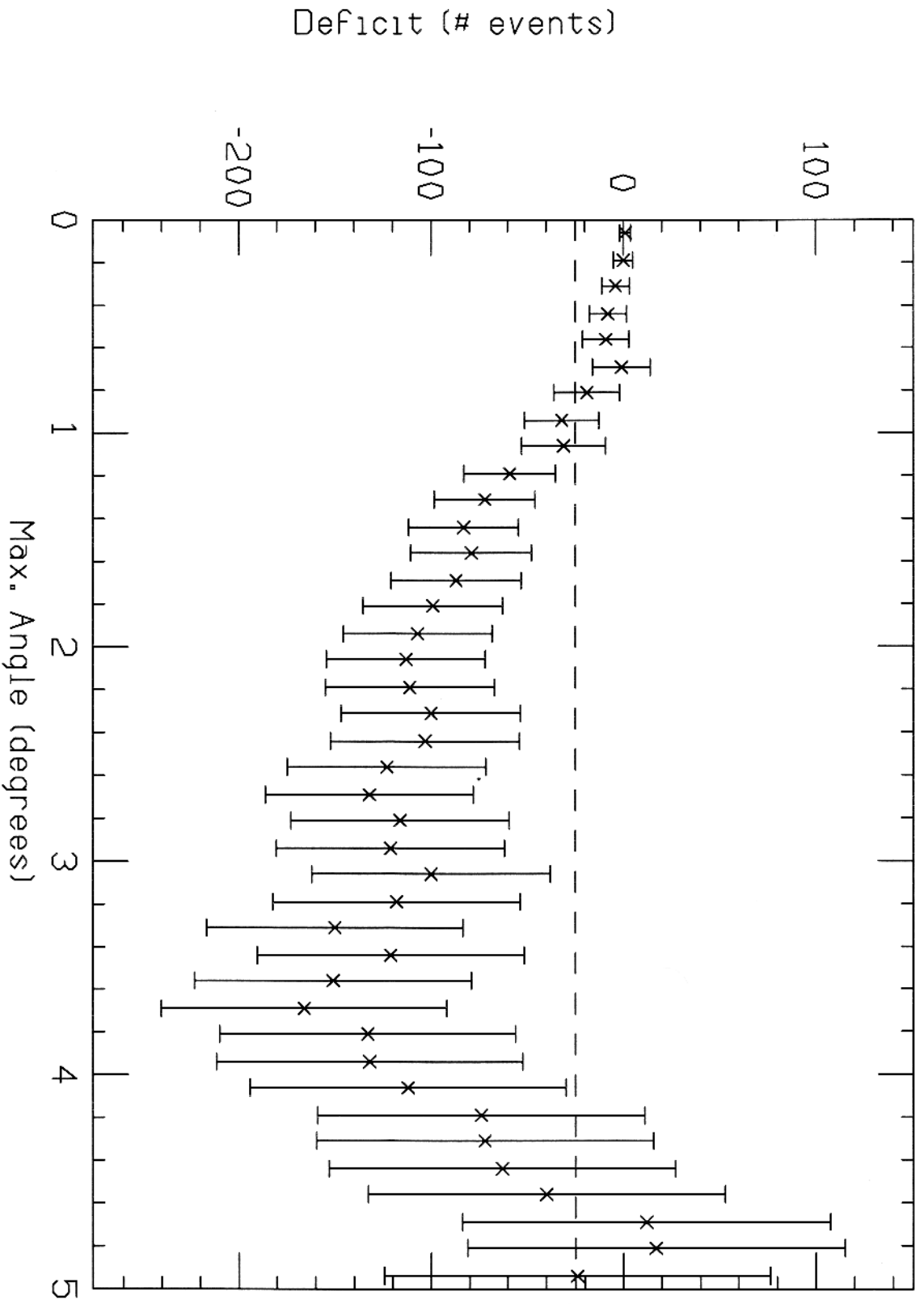
Deficit vs. Max. Angle (Figure 8b)



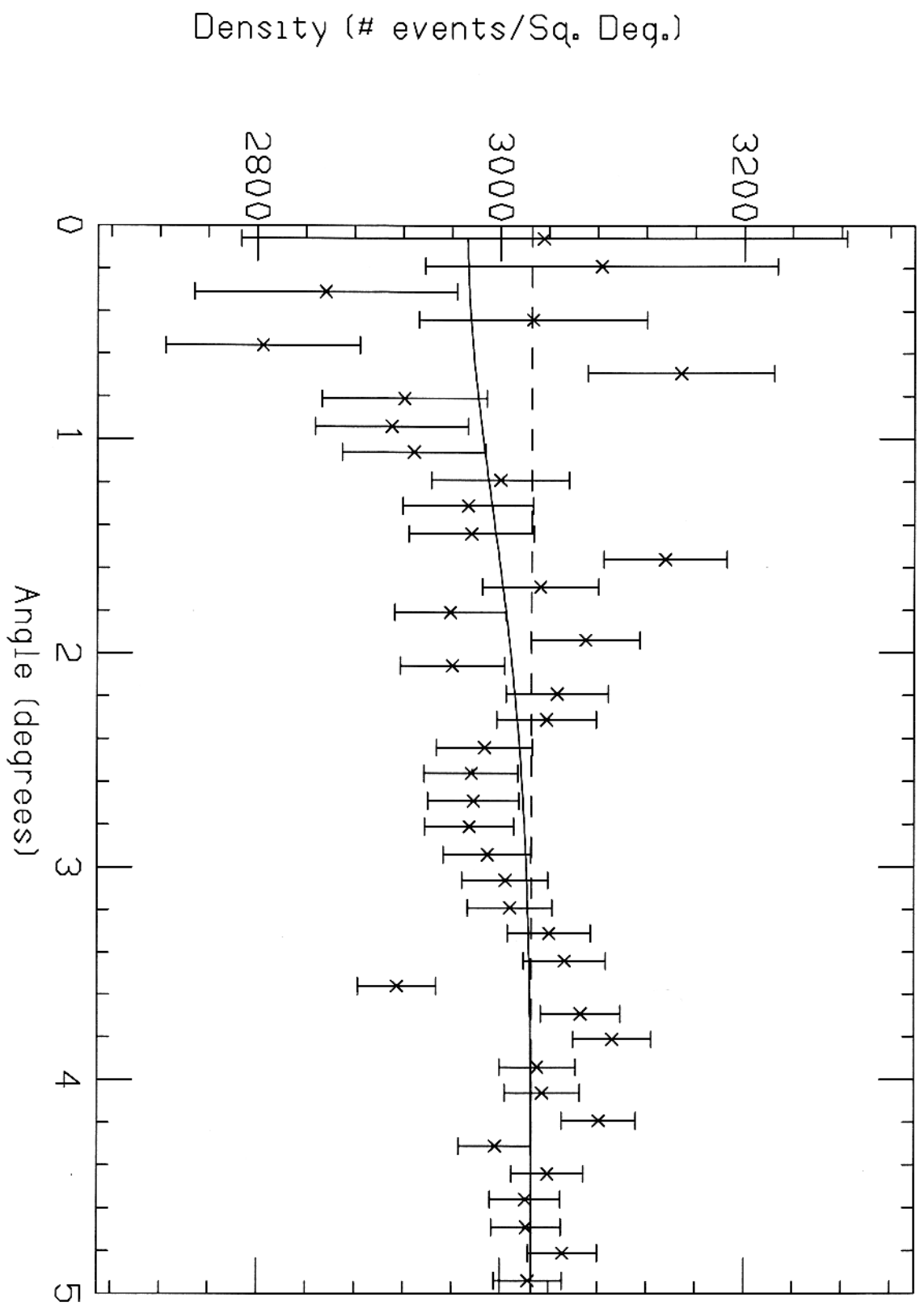
Density vs. Angle (Figure 9a)



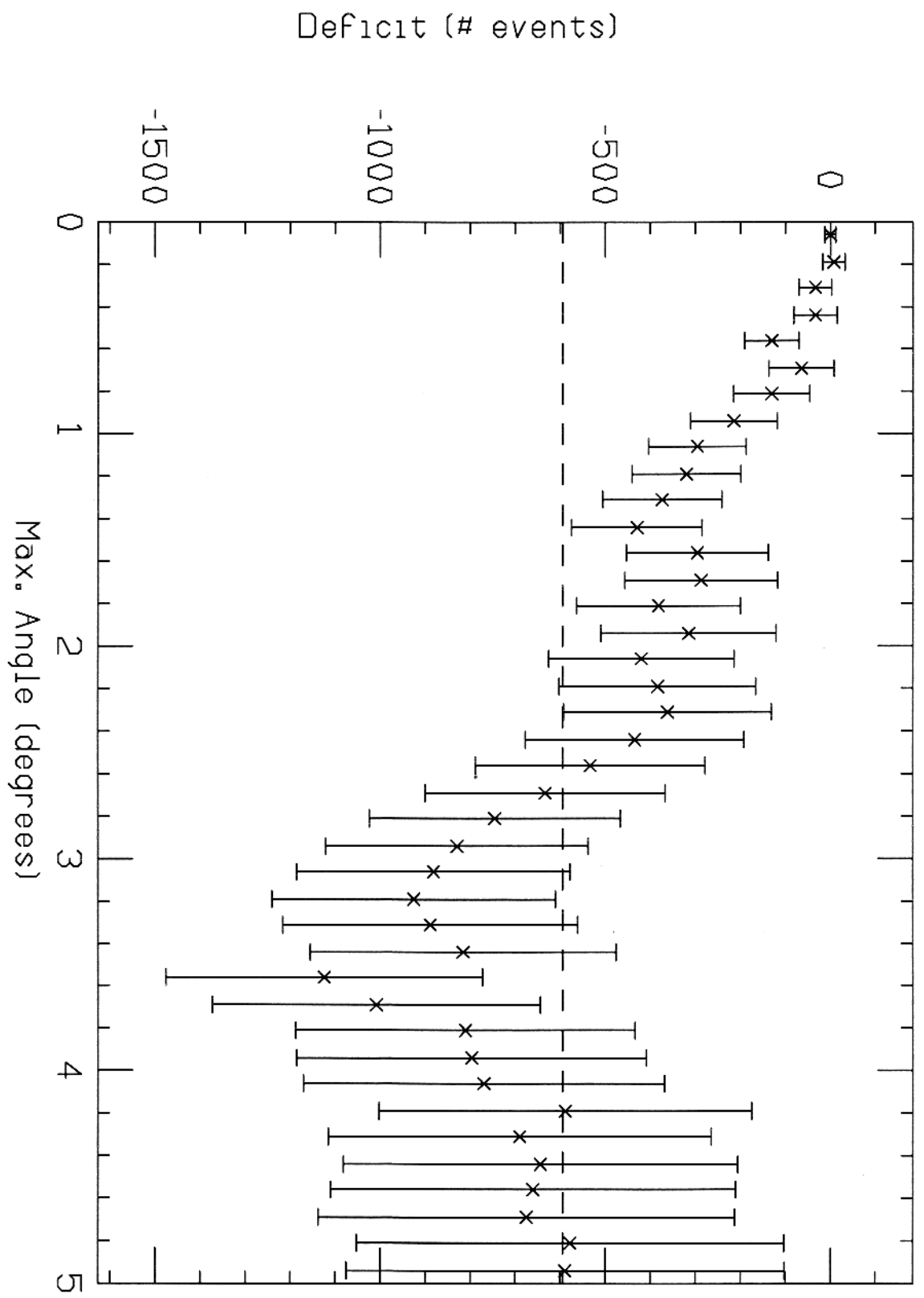
Deficit vs. Max. Angle (Figure 9b)



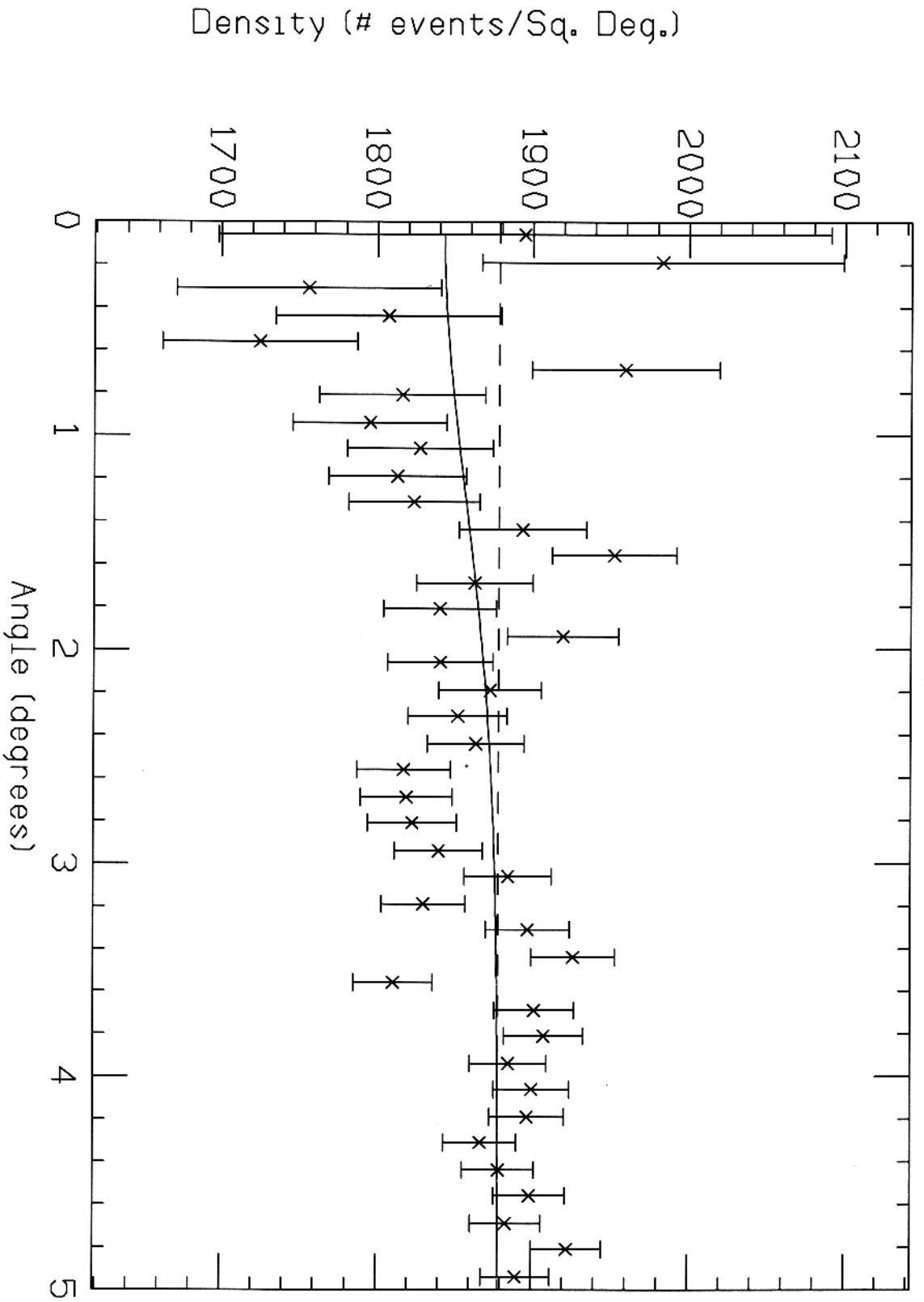
Density vs. Angle (Figure 10a)



Deficit vs. Max. Angle (Figure 10b)

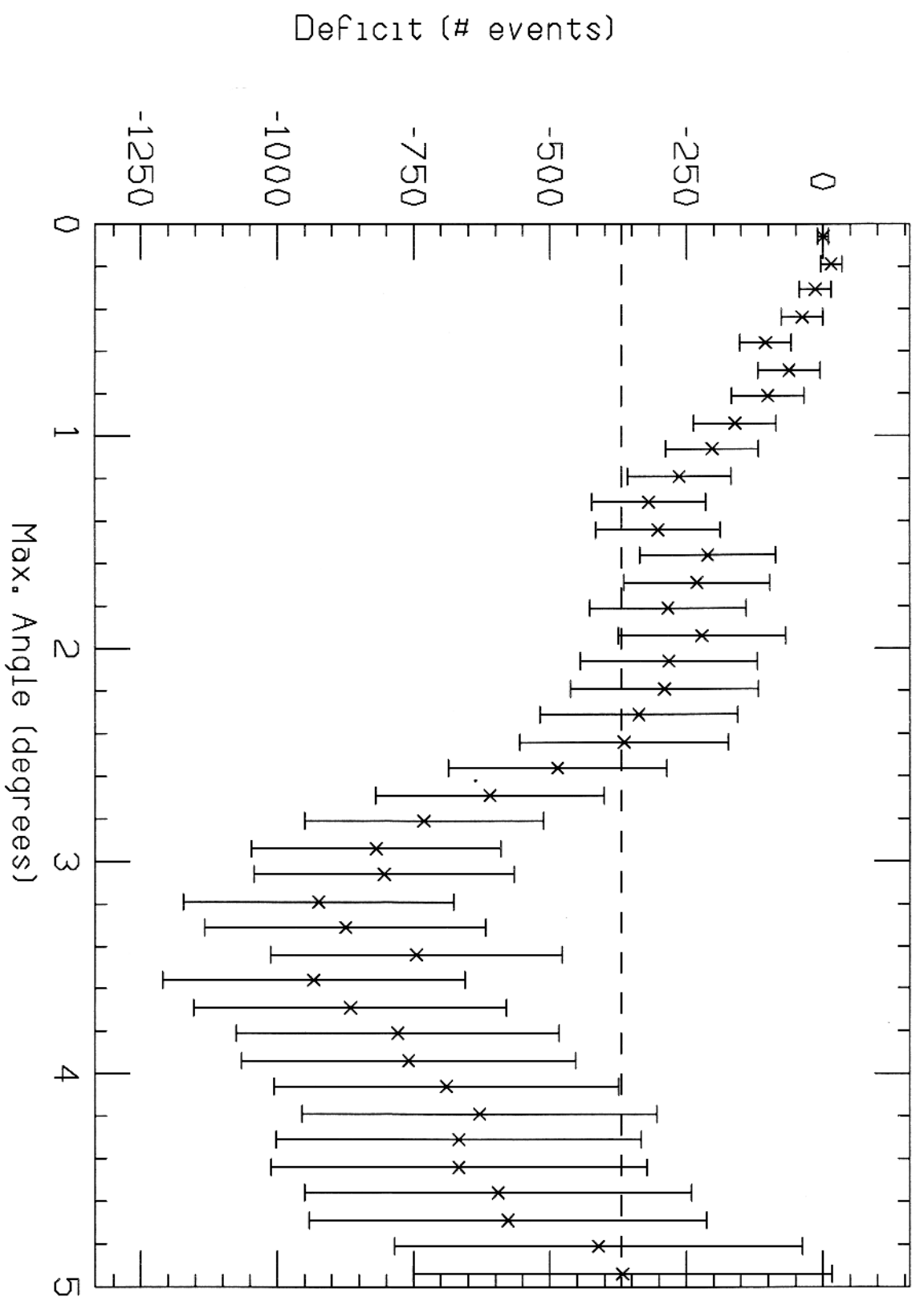


Density vs. Angle (Figure 11a)

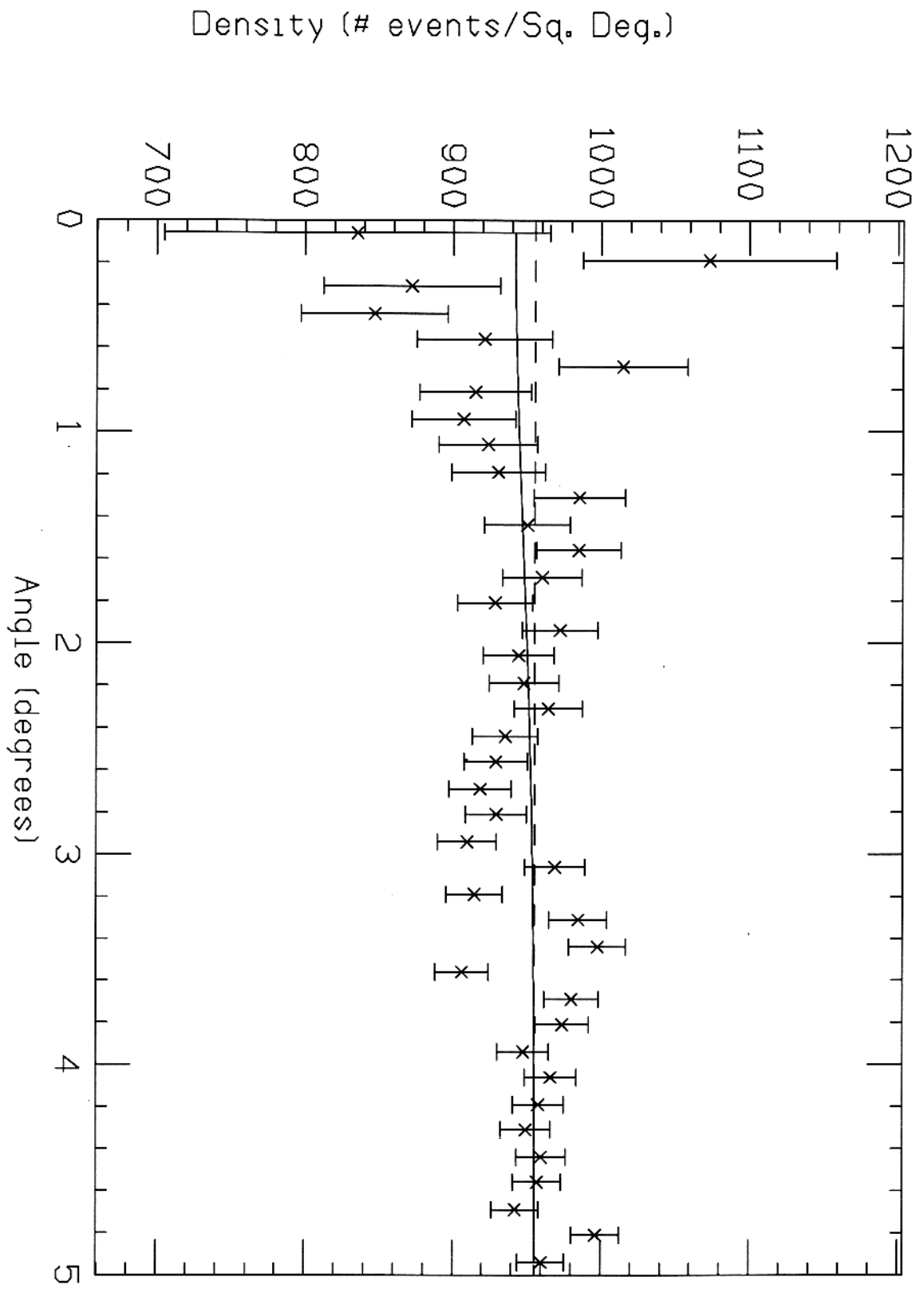




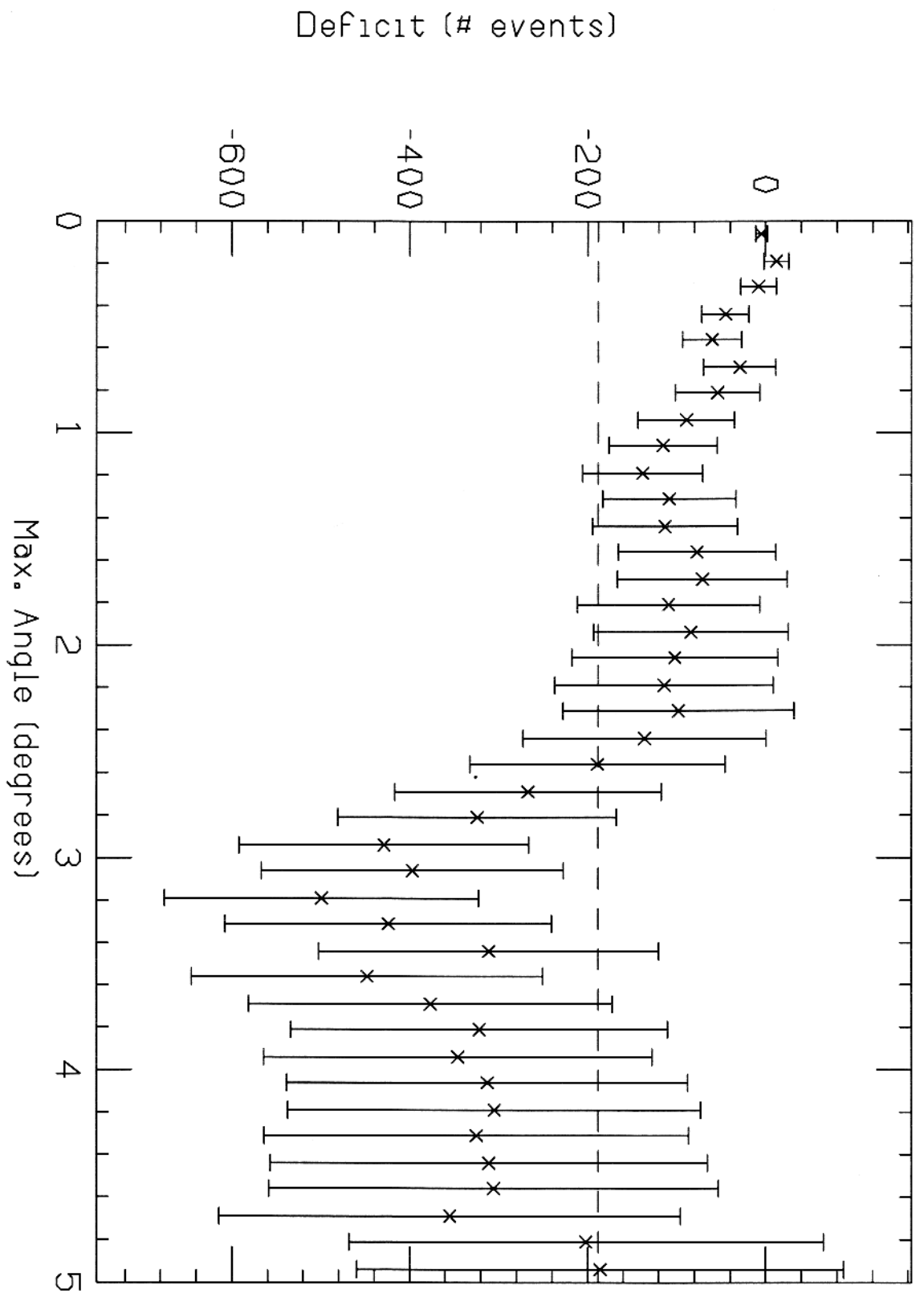
Deficit vs. Max. Angle (Figure 11b)



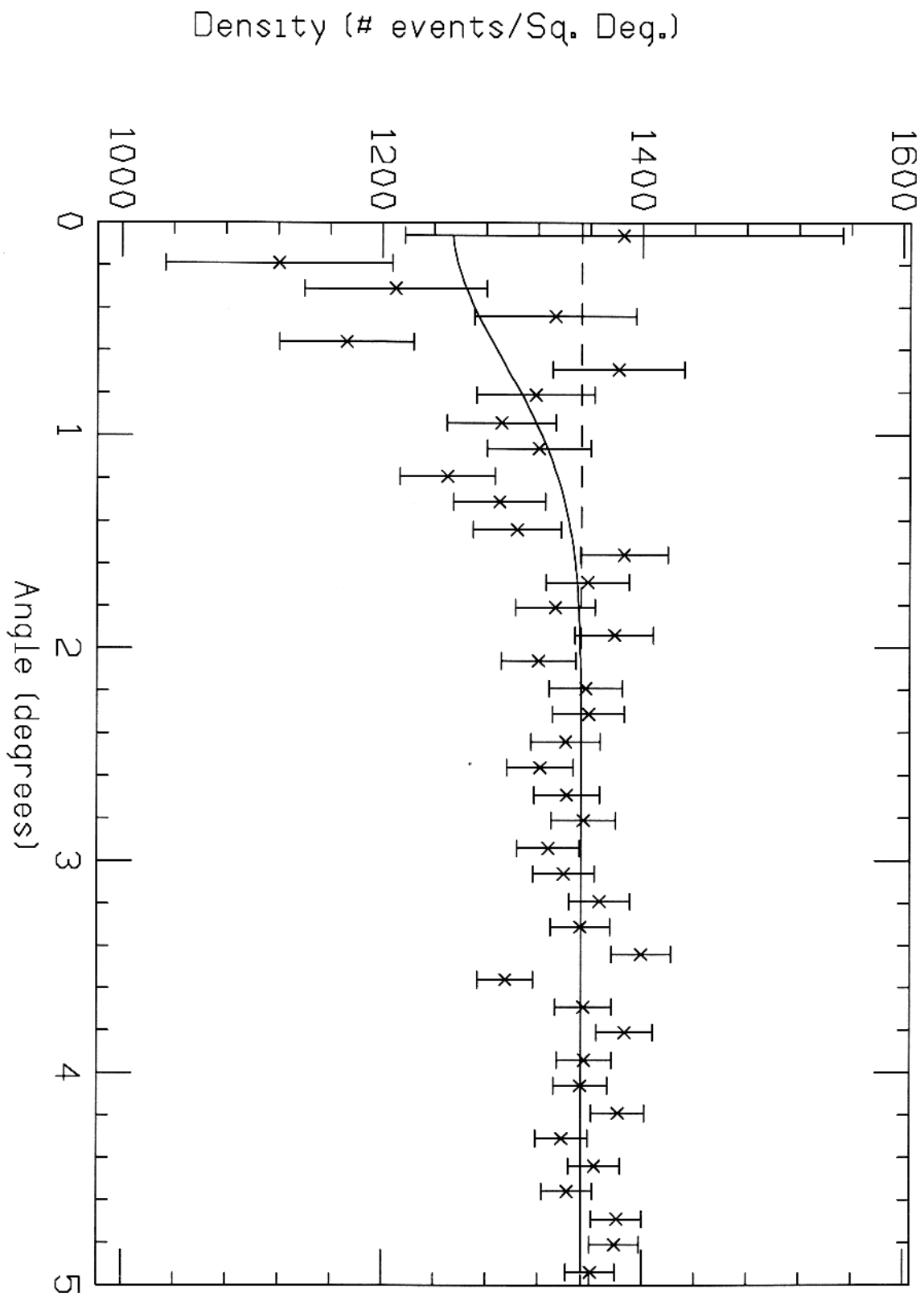
Density vs. Angle (Figure 12a)



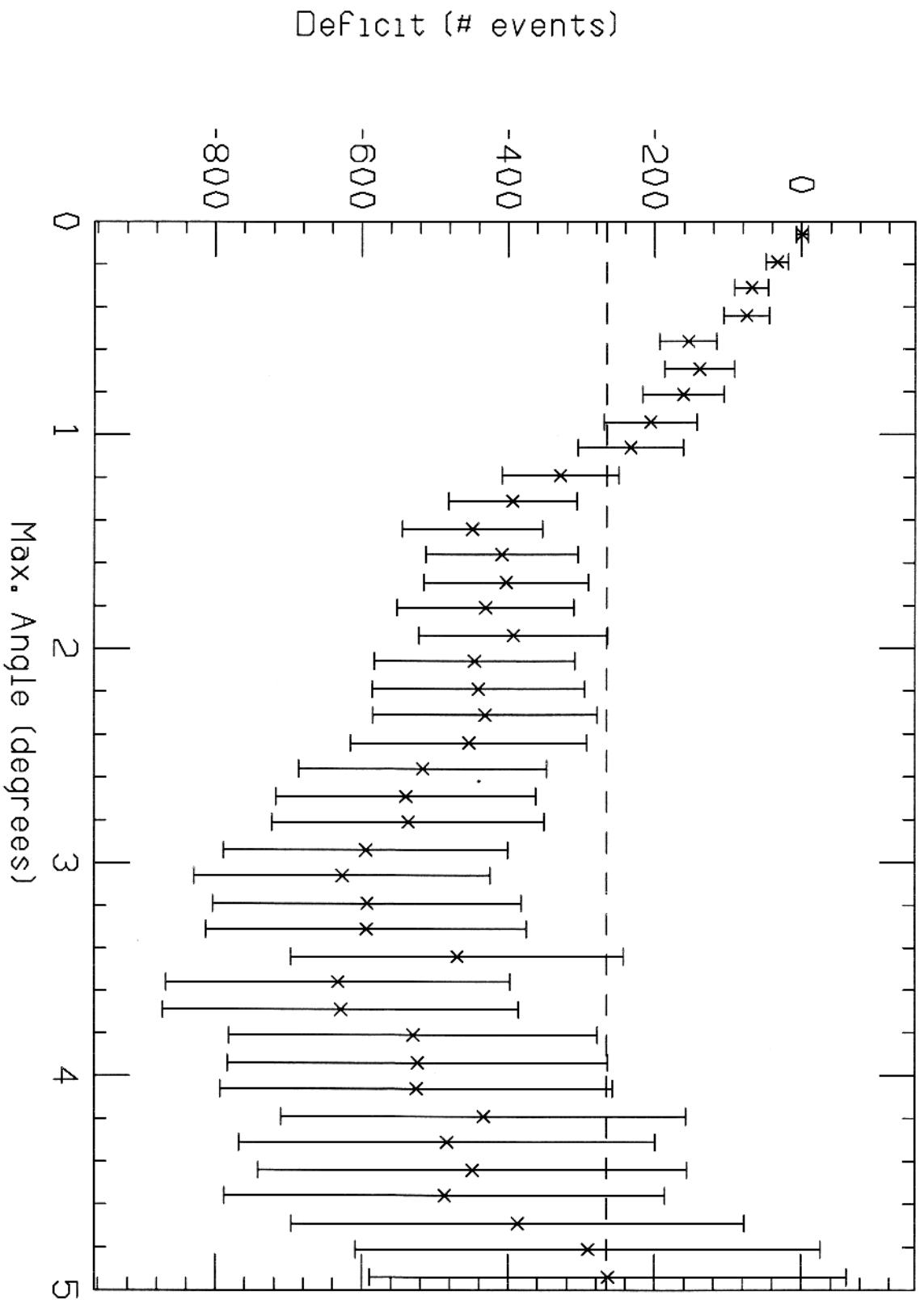
Deficit vs. Max. Angle (Figure 12b)



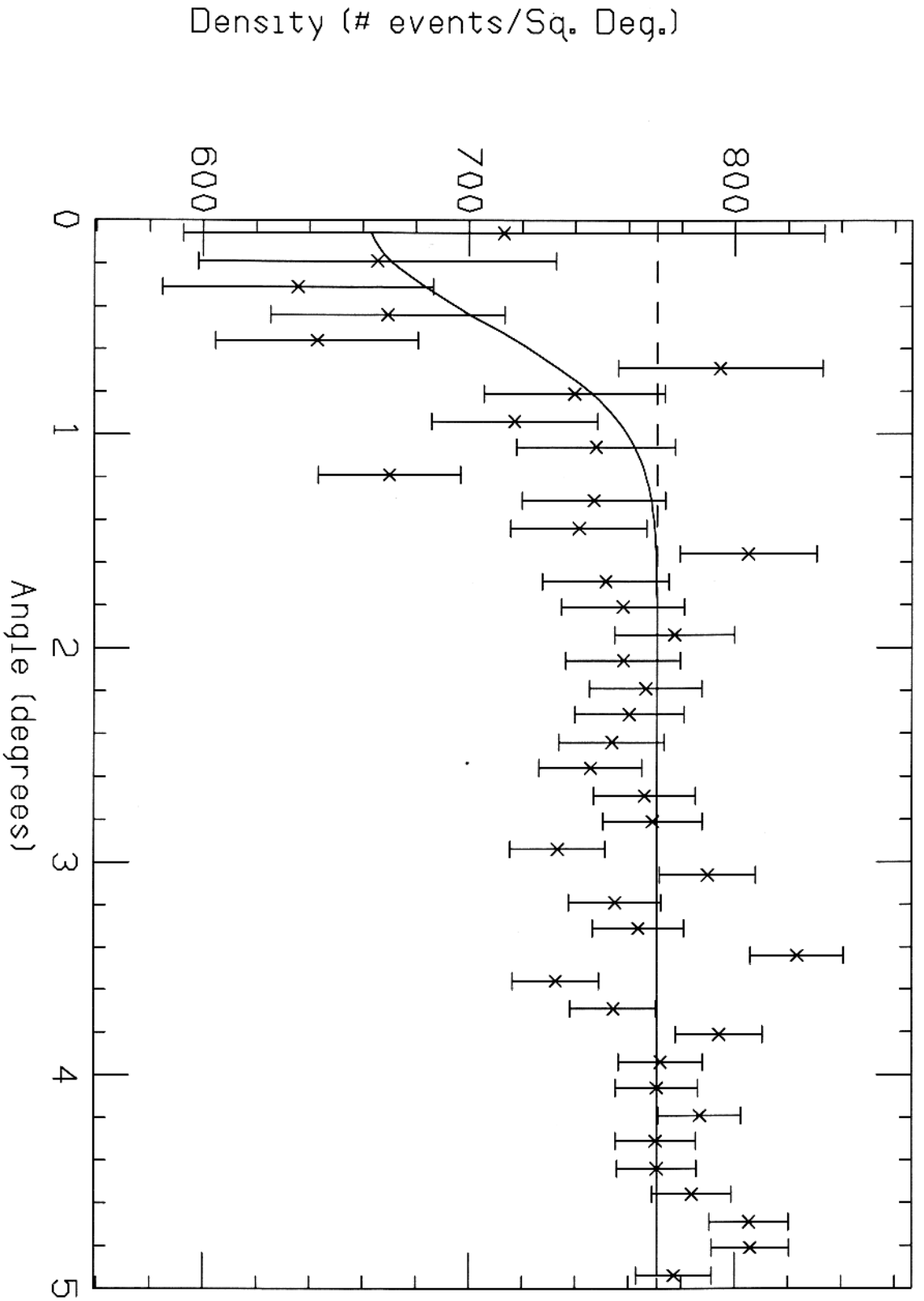
Density vs. Angle (Figure 13a)



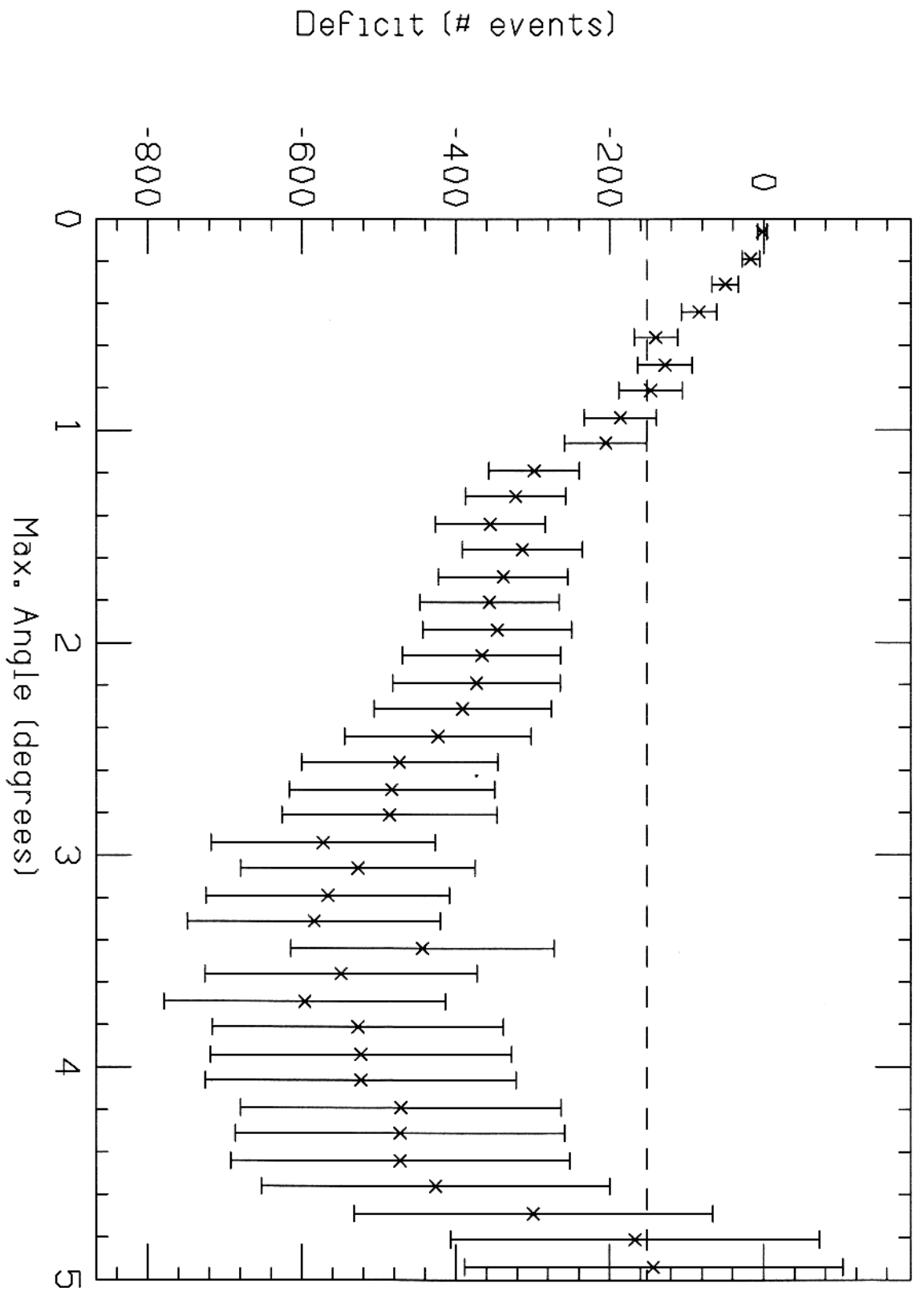
Deficit vs. Max. Angle (Figure 13b)



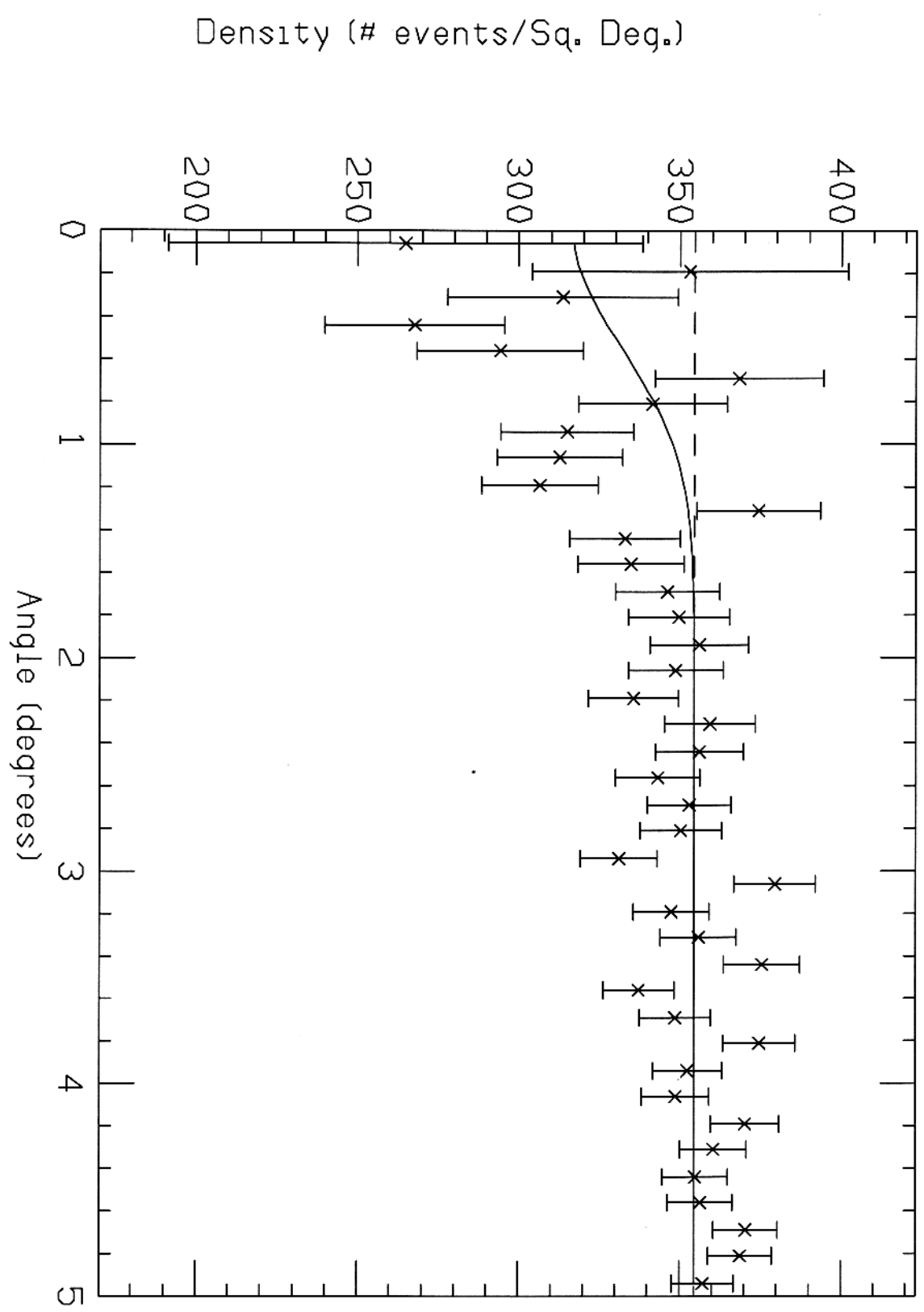
Density vs. Angle (Figure 14a)



Deficit vs. Max. Angle (Figure 14b)

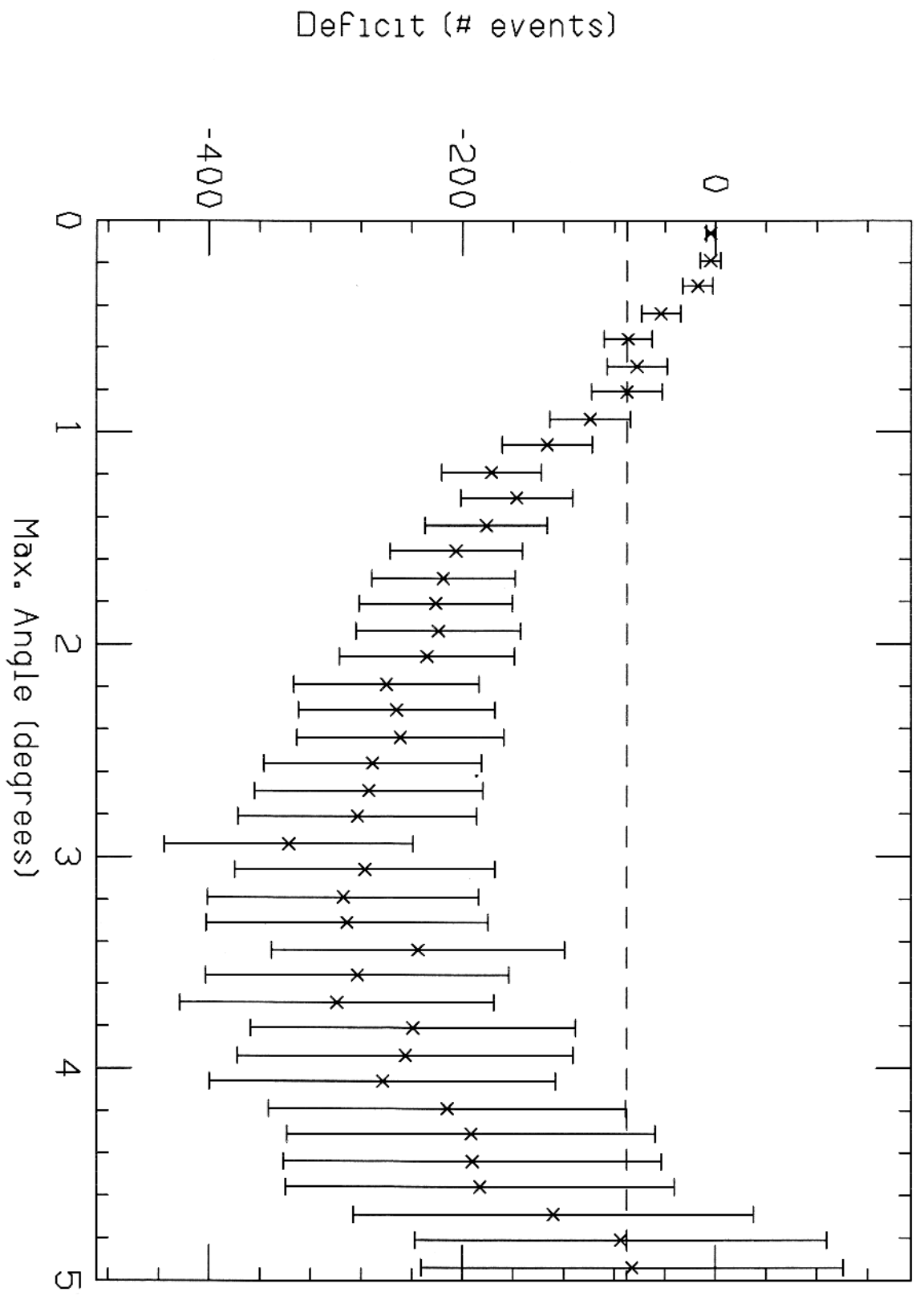


Density vs. Angle (Figure 15a)

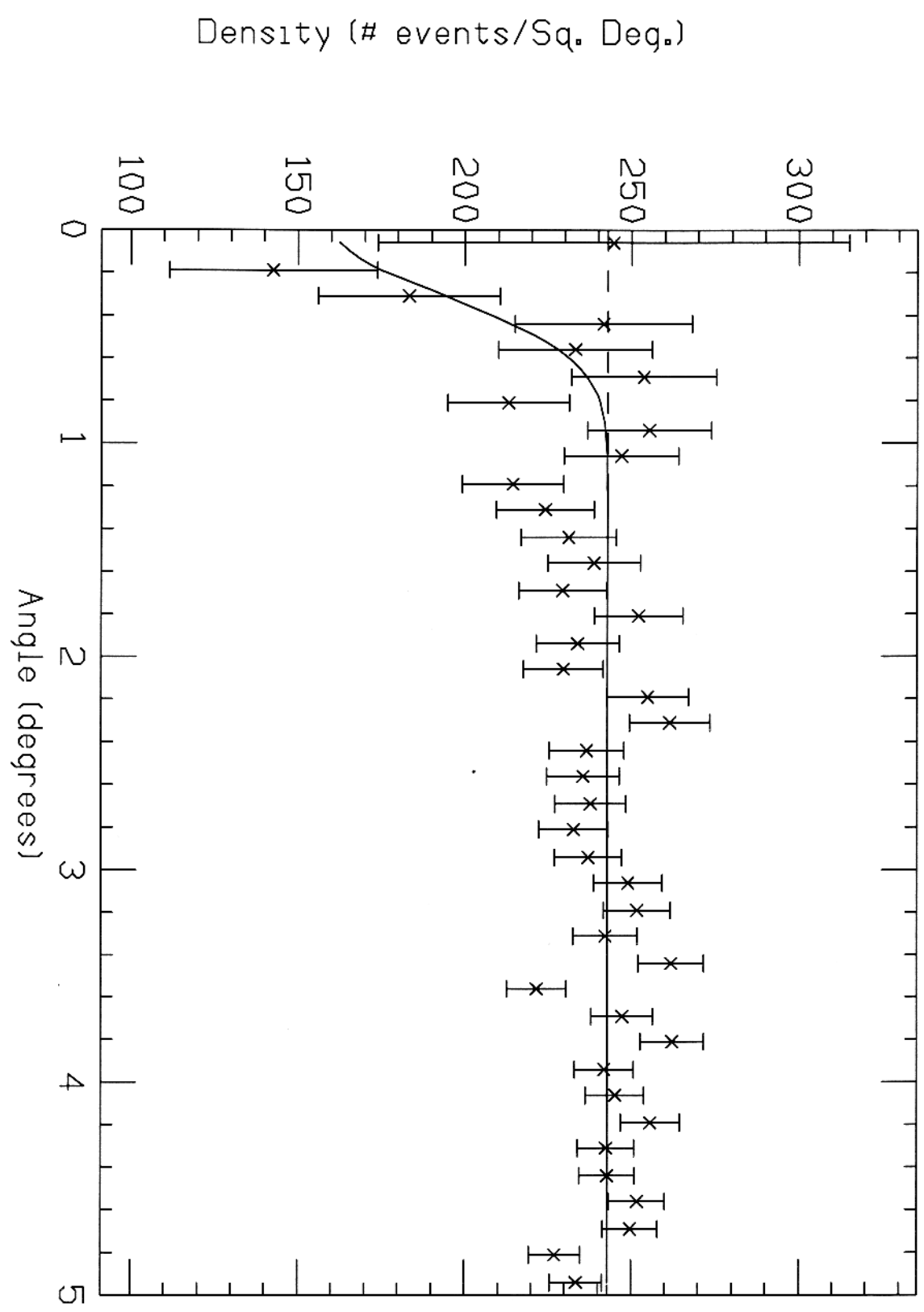




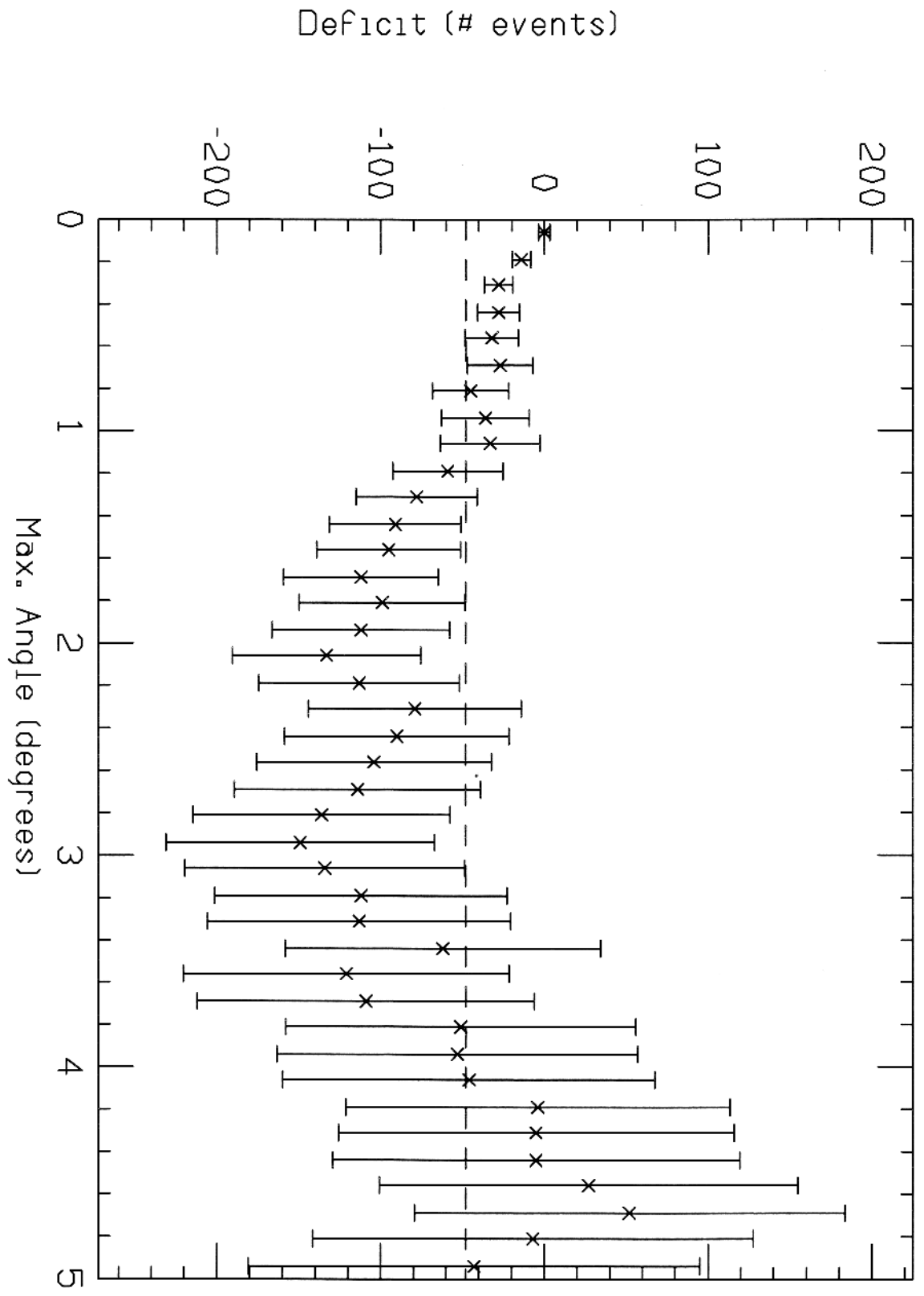
Deficit vs. Max. Angle (Figure 15b)



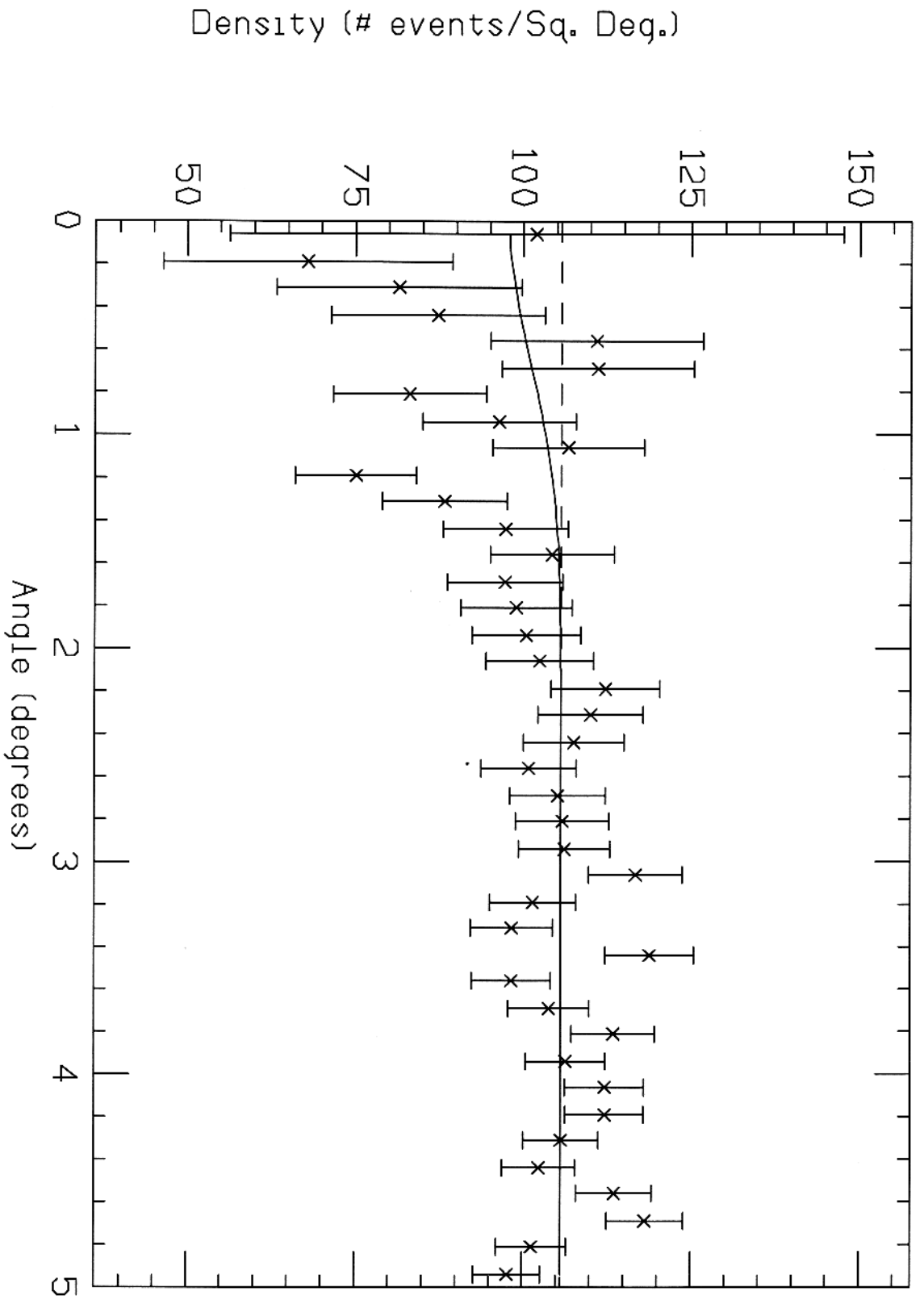
Density vs. Angle (Figure 16a)



Deficit vs. Max. Angle (Figure 16b)



Density vs. Angle (Figure 17a)



Deficit vs. Max. Angle (Figure 17b)

